Global Change Biology

Research Article

Multi-provenance assisted seed dispersal slows range contractions under climate change.

Submission ID 3d70db3c-9130-43ca-ace9-c5236e500c0b

Submission Version Initial Submission

PDF Generation 12 Dec 2025 11:25:29 EST by Atypon ReX

Authors

Dr. David Nemer
Corresponding Author
Submitting Author

Affiliations
- UMR Silva, AgroParisTech, INRAE, 54000 Nancy, France

Dr. Romain Bertrand

Affiliations
- UMR CRBE, CNRS, Université de Toulouse, Toulouse INP, IRD

Dr. Laura Chevaux

Affiliations
- UMR Silva, AgroParisTech, INRAE, 54000 Nancy, France

Mr. Mohammed Brahim

Affiliations
- Université de Caen Normandie, 14000 Caen, France

Mr. Mathieu Magnier

Affiliations
- Service Bois Agence Picardie, Office National des Forêts, 60200 Compiègne, France

Dr. Josep M Serra-Diaz

Affiliations
- UMR Silva, AgroParisTech, INRAE, 54000 Nancy, France
- Botanic Institute of Barcelona, CSIC-CMCNB, 08038 Barcelona, Spain

Files for peer review

All files submitted by the author for peer review are listed below. Files that could not be converted to PDF are indicated; reviewers are able to access them online.

Name	Type of File	Size	Page
Main text.docx	Main Document - MS Word	1.7 MB	Page 4
Figure 1.png	Figure	4.8 MB	Page 39
Figure 2.png	Figure	7.8 MB	Page 40
Figure 3.png	Figure	6.4 MB	Page 41
Supplementary 1.docx	Supplementary Material for Review	20.6 KB	Page 42
Supplementary 2.docx	Supplementary Material for Review	20.3 KB	Page 45
Supplementary 3.docx	Supplementary Material for Review	13.1 KB	Page 49
Supplementary tables and figures.docx	Supplementary Material for Review	2.2 MB	Page 50

Multi-provenance assisted seed dispersal slows range contractions under climate change.

AUTHORS: David Nemer[1], Romain Bertrand[3], Laura Chevaux[1], Mohammed Brahim[4], Mathieu Magnier[5], Josep M Serra-Diaz[1,2]

AFFILIATIONS

[1]UMR Silva, AgroParisTech, INRAE, 54000 Nancy, France
[2]Botanic Institute of Barcelona, CSIC-CMCNB, 08038 Barcelona, Spain.
[3]UMR CRBE, CNRS, Université de Toulouse, Toulouse INP, IRD,
[4]Université de Caen Normandie, 14000 Caen, France
[5]Service Bois Agence Picardie, Office National des Forêts, 60200 Compiègne, France

AUTHOR'S ORCID

David Nemer (david.nemer@agroparistech.fr; https://orcid.org/0000-0002-2140-0180, correspondence author)
Romain Bertrand (romain.bertrand2@utoulouse.fr; https://orcid.org/0000-0003-2386-9174)
Laura Chevaux (laura.chevaux@agroparistech.fr ; https://orcid.org/0000-0001-9585-1948)
Mohammed Brahim (mohammed.brahim@etu.unicaen.fr ; https://orcid.org/0009-0009-6731-4833)
Mathieu Magnier (mathieu.magnier@onf.fr; https://orcid.org/my-orcid?orcid=0009-0005-7079-2298)
Josep M Serra-Diaz (pep.serra.diaz@csic.es; 0000-0003-1988-1154)

Abstract

Rapid climate warming threatens the persistence of temperate European forests, raising urgent questions about whether traditional reliance on local seed sources remains viable. Using *Quercus petraea* in France as a model system, we combined provenance-specific species distribution models with a dynamic range-shift model (*simRShift*) to evaluate climate-informed assisted

dispersal under SSP5-8.5 from 2020-2100. We tested six regional provenances and five planting efforts within the operational seed zones framework used in French forestry.

Across all scenarios of planting efforts, *Q. petraea* experienced substantial loss of climatically suitable habitat. However, assisted dispersal markedly slowed this decline. Mixed-provenance plantings consistently outperformed local-only strategies, retaining ~2.5× more habitat by 2100. Local provenances maintained clear advantages only in climatically stable mountain regions, whereas warmer lowlands increasingly favored Atlantic, continental, and Pyrenean origins. Seed flows reorganized along aridity, continentality, and elevation gradients, producing multi-directional and altitudinally structured provenance mosaics rather than simple northward shifts. Planting effort showed strong diminishing returns, with moderate interventions (5%) capturing most of the attainable benefits.

Our results demonstrate that climate-explicit seed sourcing can substantially enhance persistence of temperate oaks under rapid climate change. Integrating assisted dispersal into an existing seed zoning framework, offers an operational pathway toward climate-adapted reforestation across Europe.

Keywords: Assisted dispersal, Seed sourcing, Local adaptation, Seed Provenance, Seed flow, Climate change, Species distribution models, *Quercus petraea*

Introduction

Forests are already experiencing rapid shifts in climate, with cascading impacts on productivity, regeneration, disturbance regimes, and mortality (Allen et al., 2010; Seidl et al., 2025; Senf et al., 2020; Trumbore et al., 2015). In Europe, warming, compound heat-drought events, and increasing disturbances are driving range contractions for many tree species, while adaptation limits are becoming apparent in several regions (Hanewinkel et al., 2013; Rigling et al., 2013). These trends challenge long-standing practices that assume local seed sources will remain best suited to future conditions and motivate climate-informed approaches to regeneration and restoration (Anderegg et al., 2020; Seidl et al., 2025; Seidl & Senf, 2024; Senf et al., 2020; Trumbore et al., 2015).

Local adaptation is well documented in forest trees. Over two centuries of common-garden and provenance trials, reinforced by genomic analyses, have revealed pronounced clines in adaptive

traits along temperature and moisture gradients, indicating that many populations are finely tuned to their local climates despite substantial gene flow (Aitken & Whitlock, 2013; Benito Garzón et al., 2019; Savolainen et al., 2007; Vitasse et al., 2009). This body of evidence established the long-standing forestry principle that "local is best," which continues to underpin seed-transfer regulations and provenance zoning, for example within the French forest seed zones framework used to define seed-source boundaries based on homogeneous characteristics of climate and soil (Guitton, 1998; IGN, 2013). Yet these same climatic clines also imply vulnerability: when the climate velocity is faster than trees can evolve or disperse (Serra-Diaz et al., 2014). In such a case, local genotypes may risk maladaptation if seed sourcing remains tied to historical conditions (Alberto et al., 2013; J. H. Pedlar et al., 2021; Rehfeldt et al., 2002).

Meta-analyses across plants show that local genotypes typically outperform foreign ones in their home sites, but also that performance advantages are context dependent and can reverse under environmental change (Hereford, 2009; Hufford & Mazer, 2003; Kawecki & Ebert, 2004; Leimu & Fischer, 2008). For trees, plasticity and high climate tolerance mean that some populations can thrive outside their place of origin, particularly along established climate gradients. This dual evidence, namely strong local adaptation and the possibility of successful transfer, defines the central dilemma for seed sourcing in a rapidly changing climate.

Assisted dispersal (AD), the intentional, human-mediated movement of species, populations, or genotypes to track shifting climates, has emerged as a prominent adaptation option (Aitken & Whitlock, 2013; McLachlan et al., 2007; J. Pedlar et al., 2012; Williams & Dumroese, 2013). Within this concept, assisted gene flow (AGF) refers to the translocation of pre-adapted genotypes within a species' range, aiming to reduce maladaptation while maintaining natural species distributions. While AGF often carries lower ecological risks than beyond-range AD, both approaches raise concerns about maladaptation to non-climatic factors, disruption of local biotic interactions, and outbreeding depression when divergent lineages interbreed (Aitken & Bemmels, 2016; Prober et al., 2015). Consequently, quantitative, spatially explicit frameworks are needed to balance benefits and risks when implementing such strategies.

In parallel, seed-sourcing concepts have diversified beyond strict local provenances. Composite provenancing mixes seed from multiple nearby sources to capture diversity and mimic natural gene flow, whereas climate-adjusted provenancing intentionally skews mixes toward sources from warmer or drier climates to hedge against directional change (Broadhurst et al., 2008; Prober et al., 2015). Although composite provenancing, mixing seed from multiple nearby sources, has

been proposed to mimic natural gene flow. Both local and climate-adjusted approaches share the premise that maintaining within-species diversity and spreading climatic risk can improve establishment and long-term persistence under uncertain futures. However, guidance on when to favor each approach remains limited by a shortage of tools coupling climatic suitability with demographic outcomes at landscape scales (Breed et al., 2019; Bucharova et al., 2019; Prober et al., 2015; Rellstab et al., 2016).

Species distribution models (SDMs) are widely used to estimate spatial climate suitability (Elith & Leathwick, 2009; Franklin, 2010; Guisan et al., 2006) and have been increasingly applied to assess assisted-migration strategies in forest trees (Hällfors et al., 2016, 2017). However, climatic suitability alone cannot predict population trajectories when dispersal, episodic recruitment, and age structure interact, factors particularly important for long-lived species (Alberto et al., 2013; J. Pedlar et al., 2012; Ste-Marie et al., 2011). To address these limitations, we combined population-specific SDMs with dynamic range-shift simulations (*simRShift*; (Bertrand et al., 2012) to quantify the joint effects of seed origin, planting effort, and topography on future persistence under climate change.

Furthermore, previous studies indicate that complex topography and vegetation can maintain more stable local microclimates than suggested by coarse regional climate projections, creating upland and topographically sheltered sites where warming rates are reduced (Aalto et al., 2018, 2022; Dobrowski, 2011). In contrast, warm low-elevation sites already show strong climatic disequilibrium for many temperate trees, with documented growth declines under recent warming (Jump et al., 2006) and increasing vulnerability of drought-related traits (Benito Garzón et al., 2019). However, climatic suitability alone does not determine future persistence; demographic processes further constrain how populations respond to change. Because oak regeneration is inherently slow and establishment probabilities remain low even under favourable climates (Clark et al., 1999), and because recruitment is ultimately limited by both seed arrival and the availability of safe microsites (Nathan & Muller-Landau, 2000), increasing planting effort is expected to improve persistence but with diminishing returns once suitable microsites become saturated.

Here, we use *Quercus petraea* in France as a case study (Figure 1). *Quercus petraea* is a widely distributed temperate oak, with high sylvicultural value and well-documented local adaptation patterns (Kremer et al., 2012). Climate change projections show a strong decline for this species by 2100 (Benito Garzón et al., 2019; Vitasse et al., 2009), but seed sourcing is restricted within the French seed zones (Figure 1). This regulatory framework corresponds to what we refer to

hereafter as the local provenance scenario. We therefore simulated the outcomes of alternative seed-sourcing strategies under future climate scenarios, varying both (i) planting effort (5%, 10%, 25%, 50%, 100% of suitable sites planted per decade), and (ii) provenance type (local versus mixed). Based on the ecological theory and empirical evidence outlined above, we hypothesized that:

(H1) Assisted seed dispersal will buffer the climate-driven decline of *Quercus petraea*, but the efficiency of planting will show diminishing returns, such that increasing planting effort yields progressively smaller gains in preserved area.

(H2) Local provenances will retain a competitive advantage only in climatically stable mountain regions, but will be outperformed by non-local sources in warmer lowlands.

(H3) Provenance selection over space and time will not follow a simple north-south or elevational gradient, but rather a multi-directional pattern emerging from interactions between climate change, topography, soil moisture, and regional climate extremes.

2. Methods

We developed a spatially explicit simulation workflow to evaluate assisted dispersal strategies using provenance-specific species distribution models (SDMs), performance metrics derived from dynamic species range simulations, and environmental suitability thresholds. The aim was to identify, per cell and per decade, the most suitable provenance (Nprovenance = 6) to assist species establishment (pixel occupancy) under future climate scenarios and assess the long-term effects of different assisted dispersal strategies on range persistence and expansion. In our simulations, assisted dispersal corresponds to planting young trees (i.e., seedlings or saplings) rather than sowing seeds, matching standard forestry practice. We used *Quercus petraea* as a case study species, with six geographically distinct source provenances.

2.1.1 Study area and species provenances

The study was conducted across Metropolitan France, excluding Corsica, which spans a pronounced climatic gradient from temperate Atlantic to Mediterranean and continental forest biomes (Figure 1).

We focused on *Quercus petraea* (sessile oak) *Matt. Liebl.*, one of the most widespread and ecologically important deciduous tree species in Western Europe. *Q. petraea* is a foundation species of temperate and sub-Mediterranean forests in France, occurring from lowland Atlantic plains to mid-elevation continental and mountain environments. In France, it covers approximately 2.1 million hectares, representing 14-15% of all metropolitan forest area, and forms extensive pure or mixed stands across most regions (NFI, 2025). At the European scale, *Q. petraea* and *Q. robur* together constitute the dominant deciduous oak complex, accounting for a major proportion of broadleaf timber volume and ecological functioning across Atlantic and continental biomes. The species' wide distribution, high ecological importance, and major silvicultural role justify its relevance as a model for assessing climate-informed seed sourcing and assisted-dispersal strategies. Beyond its ecological significance, it is also a cornerstone species in French silviculture, valued for its high-quality timber, long rotation cycles, and major contribution to both biodiversity conservation and economic forestry (Becker & Lévy, 1982; Lebourgeois, 1999). The species exhibits extensive phenotypic and genetic variation linked to local climatic conditions, with well-documented adaptive differentiation in growth, phenology, and drought tolerance (Aitken & Whitlock, 2013; Ducousso & Bordacs, 2003; Jensen, 2000; Kremer et al., 2012). This makes *Q. petraea* an ideal model for exploring the outcomes of climate-informed seed sourcing and assisted dispersal at landscape scales.

Seed origins were defined according to forest reproductive material developed by the French National Forest Inventory (NFI). This ecological zoning framework delineates regions based on biogeographic, climatic, and edaphic criteria and underpins official seed-transfer and forest-management regulations in France (Guitton, 1998; IGN, 2013).

For *Q. petraea*, we identified six representative seed-source provenances (Figure 1A), each corresponding to a distinct seed zone or cluster of adjacent regions (hereafter referred to as "Prov"): Prov 1, Atlantic Northwest, characterized by cool, humid oceanic climates; Prov 2, Northeastern Continental, with colder winters and higher thermal amplitude; Prov 3, Southwestern Atlantic, warm and subhumid; Prov 4, Massif Central, intermediate climates with pronounced altitudinal gradients; Prov 5, Alpine-Jura, cool-humid montane conditions; Prov 6, Pyrenean, warm-dry mountain climate.

These provenances encompass the major climatic and genetic diversity of *Q. petraea* across France and correspond to the officially recognized seed-provenances regions used by forestry nurseries and the *Office National des Forêts* (ONF, the French National Forest Agency). Their

geographic distribution and altitudinal ranges are illustrated in (Figure 1A), together with climatic gradients that structure their adaptive differentiation (Figure 1B).

2.1.2 Current presence-absence data

Presence-absence records of *Q. petraea* were obtained from the French National Forest Inventory (NFI), which implements a systematic 1 km × 1 km sampling grid covering the entire national territory. Approximately one-tenth of the grid nodes are surveyed annually, ensuring both spatial and temporal representativeness. We extracted all NFI plots surveyed between 2005 and 2022, resulting in 113,983 plots where *Q. petraea* was recorded as present, out of 464,747 total forest plots.

Each NFI plot follows a circular nested design, and presence was defined within a 15 m radius (709 m²) according to NFI standards. Individuals were considered present if they exceeded a diameter at breast height (DBH) of 7.5 cm, ensuring that only established trees were included while accounting for advanced regeneration.

2.2.1 Provenance climatic suitability

We developed a set of species distribution models-SDMs (Elith & Leathwick, 2009; Franklin, 2010; Guisan et al., 2006) to characterize the realized climatic niche of *Q. petraea* across Metropolitan France and to generate climate suitability layers subsequently used as inputs for dynamic range-shift simulations (*simRShift*; Bertrand et al., 2012). Two complementary biological scales were implemented: (1) a species-level SDM, calibrated on the full distribution of *Q. petraea*, representing the baseline control scenario, and (2) provenance-level SDMs, trained separately for each of the six provenances defined by the French seed zones (Prov 1-6). These provenance models capture fine-scale differences in climatic responses and were used to guide seed-source selection and planting suitability decisions.

All models were based on a consistent suite of climatic predictors previously shown to control oak distributions in France (Cheaib et al., 2011). Monthly time-series data for maximum temperature, minimum temperature, and precipitation were compiled from the CHELSA v2.1 database (Karger et al., 2017) at a 1 km spatial resolution for the period 1981-2020. The 1 km grid resolution aligns with the spatial design of the French NFI and minimizes the influence of coordinate randomization applied to preserve NFI plot confidentiality. Future climate projections for 2020-2100 were derived

214 from a single General Circulation Model (GCM), MRI-ESM2-0 under the SSP5-8.5. This climate
215 scenario represents current warming trends (O'Neill et al., 2016), and was selected based on an
216 independent evaluation conducted over metropolitan France (Supplementary Material S1), where
217 four candidate models (MRI-ESM2-0, IPSL-CM6A-LR, GFDL-ESM4, MPI-ESM1-2-HR) were
218 compared against high-resolution Météo-France observational datasets (2015-2023; >80,000
219 temperature and >97,000 precipitation records). MRI-ESM2-0 showed the lowest overall bias and
220 root mean square error across temperature and precipitation variables under both SSP3-7.0 and
221 SSP5-8.5. Because our objective is to assess biological responses rather than climate-model
222 uncertainty, we retained the single best-performing GCM, following regional model-selection
223 practice, and provided full evaluation results in Supplementary Material S1.

224 Following the BIOCLIM methodology (Xu & Hutchinson, 2011), we derived three key climatic
225 predictors representing major thermal and hydric constraints on oak distribution: mean annual
226 maximum temperature of the hottest month (TMXH), mean annual minimum temperature of the
227 coldest month (TMNC), and total precipitation of the driest quarter (PRDR). In addition to these
228 climatic predictors, we included soil pH (Coudun et al., 2006) as an edaphic covariate, as soil
229 acidity is a well-known driver of tree species distributions in France and strongly improves SDM
230 discrimination when climatic gradients alone are insufficient. Because edaphic properties change
231 over much longer timescales than climate, soil pH was treated as temporally static and assumed
232 constant under future climate scenarios. The ecological rationale for combining climatic and
233 edaphic factors is further supported by large-scale analyses of French forest communities
234 showing that both climate and substrate jointly structure species distributions, including temperate
235 oaks (Bertrand et al., 2011).

236 SDMs were implemented using two machine learning algorithms, Random Forest (RF) (Breiman,
237 2001) and Extreme Gradient Boosting (XGBoost) (Chen & Guestrin, 2016), within the tidymodels
238 framework in R (Kuhn & Silge, 2022). For each model (species-level and provenance-level), the
239 dataset was randomly split into 70 % training and 30 % testing subsets.

240 To address the imbalance between presence and absence data, a random subsampling
241 procedure was applied during model calibration to equalize the number of presence and absence
242 observations, a standard practice to improve classifier performance and reduce AUC inflation
243 (Kuhn & Johnson, 2013). Hyperparameters (see the ODMAP in Supplementary material S2 for
244 more information) were tuned via 5-fold cross-validation using a grid-search approach, optimizing
245 the area under the receiver operating characteristic curve (ROC-AUC) as the evaluation metric.

246 The final model configuration corresponded to the best-performing combination of
247 hyperparameters averaged across cross-validation folds.

248

249 Model performance was assessed using cross-validated ROC-AUC scores on the training data
250 and independently evaluated on the 30% testing subset. Final predictions corresponded to the
251 ensemble mean of Random Forest (RF) and XGBoost probability outputs, an approach shown to
252 reduce algorithmic bias and improve predictive robustness (Araújo & New, 2007; Marmion et al.,
253 2009). Model discrimination capacity was evaluated using the area under the receiver operating
254 characteristic curve (ROC-AUC) and the True Skill Statistic (TSS), computed as ensemble means
255 from RF and XGBoost outputs. All provenance-SDMs and species-SDM achieved high predictive
256 performance on testing subsets (Table S1; ROC-AUC > 0.93, TSS > 0.7), confirming that the
257 selected climatic and edaphic predictors effectively captured provenance-level environmental
258 gradients across France.

259 SDMs (both species- and provenance-levels) were projected to future decades (2020-2100, in
260 10-year intervals) under SSP5-8.5 to serve as input for the range shift dynamic simulations (see
261 below). Probability output maps, here interpreted as climate suitability, were for each provenance
262 within and across seed zones per decade, enabling the dynamic 10-yr evaluation of assisted
263 dispersal strategies under future climates.

264 Metadata for all SDMs follow the ODMAP standard (Zurell et al., 2020) and are available in the
265 Supplementary material S2.

266

267 **2.2.2 Dynamic range shift simulations**

268 We used the *simRShift* (SRS) model (Bertrand et al., 2012) to simulate climate-driven forest
269 provenance dynamics and spatial range shifts. SRS is a process-based, cohort-explicit model
270 that tracks the number of juveniles, mature individuals, and mortality within each 1-km cell over
271 decadal time steps.

272 At each time step, provenance change results from reproduction, establishment, dispersal,
273 growth, and mortality, which are modulated by climatic suitability and local stand conditions. In

this study, growth, mortality, reproduction and establishment are driven by the climatic suitability from SDM outputs. Species-specific life-history traits such as age of maturity, lifespan, dispersal distance, and reproductive periodicity (masting) are explicitly integrated, making the model particularly suited to simulate long-lived, slow-dispersing species such as oaks, species-specific parameters can be found in (Table S2). Dispersal probability in *simRShift* depends on both species traits and land cover (NFI). Following Bertrand et al. (2012), we assumed full dispersal in forested cells (P = 1), reduced dispersal across semi-forested mosaics (P = 0.75 for forest < 30 %), and limited dispersal through non-forest areas (P = 0.5). This approach captures the known fragmentation effects on acorn dispersal and regeneration. We assumed no major land-use change during the 21st century, constraining potential colonization to existing forest and semi-forest habitats.

Each simulation was run at 1-km spatial resolution over the period 2020-2100 in 10-year time steps, representing decadal averages of climate conditions. We restricted simulations to cells with ≥30 % forest cover and added isolated patches containing National Forest Inventory (NFI) presences in mixed forest-agriculture mosaics, ensuring that all known occurrences were included in the initial distribution.

The initial distribution of *Q. petraea* was delineated using the alpha-hull method (α = 0.03; (Pateiro-López & Rodríguez-Casal, 2010), which flexibly defines species range boundaries while excluding spatial outliers (Serra-Diaz et al., 2024). This geographic approach, independent of the SDMs, ensures realistic initialization of the range even where NFI sampling is sparse (Boonman et al., 2024; Guo et al., 2023). Cells containing known presences but excluded by the alpha-hull, for instance in isolated patches in agriculture-forest mosaics, were added to the initial range.

Initial age structure and cohort density per cell were derived from NFI plots; missing values were imputed using a k-nearest neighbor (kNN) approach (Kowarik & Templ, 2016), based on environmental similarity (elevation, soil pH, ecoregion, and bioclimatic predictors). This method has been successfully applied to reconstruct forest age and composition for dynamic simulation modeling (Beaudoin et al., 2018; Serra-Diaz et al., 2018).

We simulated three scenarios of species assisted dispersal:

(1) No assisted dispersal (SRS-control)

Which serves as a baseline to compare against assisted strategies. This baseline run used the species-wide SDM of *Q. petraea* to project range dynamics under climate change without any planting intervention. It simulated natural recruitment, dispersal, and mortality from 2020 to 2100, providing a control against which to quantify range contraction and persistence.

(2) Planting simulations (SRS-planting for mixed provenances)

This scenario introduced assisted-dispersal planting interventions every decade from 2030 to 2090. It consists of two sub-steps:

Provenance-performance simulations (SRS-performance)

To quantify the intrinsic performance of each regional provenance (Prov 1-6), we ran separate simulations (SRS-performance) using their corresponding provenance-specific SDMs as climatic input. Each simulation produced decadal outputs describing the number of new juveniles, mature trees, and mortality per cell. From these, we computed performance metrics for each provenance at each decade (e.g., 2030-2040): Maturation success = (new mature individuals in 2040) / (initial juveniles in 2030), Reproductive success = (new juveniles in 2040) / (initial matures in 2030), Persistence ratio = (total individuals in 2040) / (total in 2030), and Mortality rate = (deaths in 2040) / (total in 2030). These indices were combined into a composite performance score (*perf_score: Maturation success score* + *Reproductive success score* + *Persistence score* + *Mortality score)* for each provenance and decade.

Decadal planting decisions

Then, for each time step, we combined the environmental suitability score (i.e., the predicted probability of occurrence from the provenance-specific SDMs; envS_score) and the performance score (from SRS-performance) using an equal weighting scheme. The final suitability index was therefore computed as*: Final_score = 0.5 × perf_score + 0.5 × envS_score.*

The provenance with the highest *Final_score* in each cell was selected as the best-performing provenance. Planting was permitted only where environmental suitability ≥ 0.6 and site fertility ≥ 0.6 (details on site fertility can be found in supplementary material S3), and in cells where the species was absent (to align with assisted dispersal principles). The threshold of 0.6 was chosen

because values above this level represent moderate to high climate suitability, ensuring that planting occurred only in locations where establishment and persistence were likely to be maintained. New cohorts of juveniles (age = 5 years) coming from the best provenance were added to eligible cells, with planting effort varying by scenario (5 %, 10 %, 25 %, 50 %, 100 % of suitable cells). These cohorts were introduced into the model's juvenile layer and simulated from year t to t + 10 (e.g., 2030-2040), after which the planting-selection-simulation loop was repeated for each subsequent decade until 2100.

Because planting decisions are based on provenance-SDM suitability, but SRS trajectories follow the species-level SDM, we applied a post-hoc ecological filtering step to enhance ecological realism and address conceptual concerns to retain only planted cells where establishment succeeded. For each decade, we compared newly planted cells (e.g. 2090 plantings) with *simRShift* outputs in the next decade (e.g. presence in 2100), retained only planted cells where establishment successfully persisted, and excluded non-persistent cells from maps and summary statistics.

Specifically, we compared planted cells (e.g., in 2090) with predicted presence from *simRShift* in the subsequent decade (e.g., 2100) and removed non-persistent cells from the visualizations and downstream analyses. This step reconciles the use of population-level SDMs (used for selecting where to plant) with the species-level SDM used within *simRShift* simulations. The filtering guarantees that only realistic, demographically viable planting efforts are considered. On average, over 85-90% of planted cells persisted to the next decade, with minor variation across time and planting effort (see Supplementary Figure. S1). Provenance-level survival rates were consistent across space and time (e.g., Q. petraea 5: 90.1%, Q. petraea 4: 76.4%, Q. petraea 6: 75.3%, Q. petraea 3: 83.0%; see Supplementary Figure. S2).

(3) Assisted dispersal using local provenances (SRS-planting local)

This scenario mirrors the mixed-provenance planting framework but restricts planting strictly to the local provenance of each seed zone. No non-local provenance was allowed to be selected, representing a traditional "local-only" seed-use strategy with no assisted dispersal allowed across seed zones.

Because *simRShift* includes stochastic dispersal and mortality processes, each simulation was repeated 50 times to capture internal variability. Outputs were summarized as mean predicted presence, recruitment, and mortality across replicates.

2.2.3 Statistical analyses of planting efforts and provenance-environment sorting

All statistical analyses were done using R ver. 4.3.2 (https://www.R-project.org/). To evaluate whether planting treatments produced significantly different outcomes, we analysed two complementary aspects of the simulation outputs: (i) planting treatment effects on preserved area and efficiency (efficiency, calculated as the gain in additional occupied cells compared to baseline without planting, relative to the number of cells planted per decade), and (ii) environmental differences among planted provenances.

Planting treatment effects on preserved area and efficiency

We tested whether planting effort (5%, 10%, 25%, 50%, and 100% of suitable cells planted per decade) significantly influenced preserved area and efficiency using linear mixed-effects models (LMMs). Because the dataset contains repeated observations for multiple years (2030-2100), year was treated as a random intercept to account for temporal non-independence, while planting percentage was treated as a fixed effect. Models were fitted in R using restricted maximum likelihood (REML) with *lmer* (lme4), and denominator degrees of freedom and p-values were obtained using the Satterthwaite approximation (*lmerTest*). Estimated marginal means and Tukey-adjusted pairwise contrasts were computed with *emmeans*.

Environmental differences among provenances

To assess whether planted provenances were preferentially assigned to distinct climatic environments, we analysed variation in four environmental variables at planting locations: mean annual maximum temperature of the hottest month (TMXH), mean annual minimum temperature of the coldest month (TMNC), total precipitation of the driest quarter (PRDR), and elevation. For each variable, we fitted an LMM with provenance as a fixed effect and planting year as a random intercept to account for decadal differences in the climate. Provenance differences were tested using Satterthwaite-adjusted F-tests, and significant pairwise contrasts were identified using Tukey-corrected estimated marginal means.

Results

Across all scenarios, *Quercus petraea* exhibited a sharp contraction of climatically suitable habitat through the 21st century (Figure 2A). This effect is evident regardless of the planting effort . Increasing planting effort enhanced total preserved area, but with pronounced diminishing returns (Figure S3-S7). Final presence rose from ≈ 102 × 10^3 ha at 5 % effort to ≈ 189 × 10^3 ha (10 %), 411 × 10^3 ha (25 %), 683 × 10^3 ha (50 %), and 1018 × 10^3 ha (100 %). Efficiency declined monotonically with effort, indicating that low-effort strategies were most cost-efficient, whereas higher efforts maximized total persistence (Figure S6, S7). These patterns were statistically confirmed by linear mixed-effects models (Table 1), planting percentage had a highly significant effect on both preserved area and efficiency (both $p < 0.0001$). Preserved area increased monotonically with planting effort, whereas efficiency decreased significantly from 5% to higher planting efforts (all Tukey-adjusted $p < 0.0001$), demonstrating clear diminishing returns, and revealing a trade-off between total preserved area and efficiency (Table 1). We thus retained the 5% planting effort for subsequent analyses, as it represents a realistic and cost-efficient level for large-scale implementation.

Without planting, the projected presence area declined from roughly 3,762 × 10^3 ha in 2030 to 2 × 10^3 ha by 2100. Active planting substantially slowed this decline, but mixed plantings retained a consistently larger presence, reaching ≈ 102× 10^3 ha by 2100 compared with ≈ 46× 10^3 ha under local seed use and only ≈ 2 × 10^3 ha without planting (Figure 2B). Early in the 21st century, local and mixed strategies showed similar distributions, yet from 2060 onward mixed origins supported broader, more continuous forest cover , particularly in central and eastern France.

The composition of seed provenance varied strongly among seed zones (Figure. 3A, B). The Alpine-Jura region (Zone 5) remained entirely self-sourced (Prov 5, 100 % local; Figure 3A, B, C). Statistical analyses showed that provenance 5 was assigned to the coldest and wettest environments among all provenances (TMNC and PRDR LMMs, both $p < 0.0001$; (Table 2).

In contrast, the Massif Central (Zone 4) became a major sink (Figure 3A, B, C), integrating local (Prov 3, ≈ 35 %), northeastern continental (Prov 2, ≈ 39 %), Pyrenean warm-dry (Prov 6, ≈ 19 %), and warm-dry southwestern Atlantic origins (Prov 3, ≈ 7 %) donors, each occupying distinct altitudinal belts. At high elevations (> 1100 m), local, northeastern continental, and Pyrenean provenances coexisted, whereas warm-dry southwestern Atlantic origins (Prov 3, ≈ 7 %) were restricted to intermediate plateaus between 391 & 1100 m (Figure 3A ,B ,C).

The northeastern region (Zone 2, Vosges/Alsace/Champagne) displayed a similarly structured mosaic, combining local (Prov 2,≈ 74 %) + Alpine genotypes (Prov 5, ≈ 5 %) concentrated in the Vosges Mountains, with Atlantic donors (Prov 3,≈ 20 %) restricted to warmer lowlands (95.9-398 m), illustrating fine-scale differentiation between montane and planar environments (Figure 3A, B, C).

The climate sorting pattern in the northeastern region (Zone 2, Vosges/Alsace/Champagne), and the Massif Central (Zone 4), aligns with our statistical results, which showed that Prov 3 was planted in the warmest sites in lowlands (highest TMXH and TMNC values, (Table 2), whereas Prov 2, 4, 5, and 6 occupied cooler, wetter uplands ($p < 0.0001$).

In the Pyrenean region (Zone 6), approximately 45 % of planted cells originated from the Massif Central provenance (Prov 4), 42 % from the continental northeastern provenance (Prov 2), and 13 % from the local Pyrenean provenance (Prov 6). These three origins co-occurred within a narrow elevational belt between ~1050 and 2100 m.

Oceanic north-western France (Zone 1) drew predominantly from south-western Atlantic provenances (Prov 3, ≈ 95 %), reflecting climate matching along an oceanicity gradient, while the south-western region lost climatic suitability and ceased to receive planting effort by late century (Figure 3A, B, D).

Discussion

Our simulations demonstrate that climate-informed assisted dispersal can partially mitigate the climate-driven decline of *Quercus petraea*, confirming key aspects of our initial hypotheses. As predicted by H1, range persistence increased with planting effort, but with strong diminishing efficiency. In line with H2, local adaptation persisted mainly in climatically stable mountain regions, whereas in warmer and drier lowlands, mixed seed provenance enhanced persistence by combining local and warm-adapted provenances. Consistent with H3, assisted dispersal produced multi-directional rather than simple latitudinal seed flows, reflecting climatic matching along aridity, continentality and elevation gradients. Together, these findings highlight how local adaptation, spatial reorganization and planting effort jointly determine the long-term effectiveness of assisted dispersal under future climates.

Assisted dispersal effort mitigates but does not prevent the decline of *Quercus petraea*

Our results show that assisted migration, regardless of the specific seed provenance, can substantially slow the projected climate-driven contraction of *Quercus petraea* compared with natural dispersal alone. Under a no-planting scenario, the species retained only ≈2 × 10^3 ha by 2100, whereas any planting strategy maintained more area (Figure 2B). This demonstrates that planting, when implemented strategically by forest managers, can meaningfully buffer the rate of decline and prolong the persistence of *Q. petraea* under climate change. The challenge then becomes not whether to plant, but how to allocate planting effort and which provenances will maximize both persistence and genetic resilience.

Building on this overarching result, our simulations confirm the main hypotheses guiding our analysis. As predicted by H1, In our simulations, total range persistence increased monotonically with planting effort but showed clear diminishing efficiency, reflecting the expected saturation of suitable microsites once the most favorable habitats are occupied. Around 5 % of planting effort would likely capture most of the attainable gains, while doubling effort beyond that could produce only modest additional benefits.

This non-linear relationship suggests that moderate planting levels (≈ 5-10 %) could offer an optimal trade-off between total persistence and operational feasibility. Beyond this range,

468 increasing planting effort would yield in sharp diminishing ecological returns while dramatically
469 increasing logistical and financial demands. In practice, planting more than 5-10 % of suitable
470 microsites per decade would likely exceed realistic nursery production, labor capacity, and
471 budgetary constraints for most European forest agencies. Thus, low-effort strategies remain not
472 only the most efficient per planted cell but also the most plausible to implement at scale, whereas
473 higher efforts (≥ 25-50 %) maximize absolute area retained but may be impractical given current
474 reforestation capacities.
475
476 Similar diminishing returns have been observed in empirical reforestation and assisted-dispersal
477 programs, where high-density or large-scale plantings increased cost and logistical burden
478 without proportionate ecological gain (Williams & Dumroese, 2013). Strategic, moderate
479 investments could prove to be sufficient to achieve most survival and adaptation benefits,
480 particularly when genetic diversity and site selection are optimized (Alfaro et al., 2014). Together,
481 these findings suggest that moderate, spatially targeted planting efforts could deliver substantial
482 persistence benefits under climate change while remaining feasible within operational and
483 financial constraints.
484
485 Spatially, increasing planting effort would likely expand the footprint of mixed-origin forests
486 outward from mountainous and continental cores into adjacent lowlands, reflecting the
487 progressive saturation of suitable microsites within the area (Figure S3, S4). These dynamics
488 suggest that early planting in climatically secure regions could stabilize core refugia, while
489 incremental expansion toward transitional zones might help maintain connectivity under ongoing
490 change.
491 **Local and mixed provenances are an option in many regions**
492
493 Local origins retained advantages in topographically buffered regions, confirming long-standing
494 evidence for local adaptation in forest trees (Aitken & Whitlock, 2013; Savolainen et al., 2007).
495 The Alpine-Jura region remained entirely self-sourced through 2100 (Figure 3A,B). Our statistical
496 analyses showed that provenance 5 was consistently assigned to the coldest and wettest
497 environments among all provenances, indicating that its climatic niche remains well aligned with

future conditions. Likewise, in the high Massif Central (> 1100 m), local provenances were the second most dominant in persistence where microclimatic buffering could have maintained conditions similar to historical baselines (Figure 3A,B).

Elsewhere, local-only and mixed provenances performed similarly until 2060, after which locals declined faster in lowland and continental zones (Figure 2B). This pattern aligns with meta-analyses showing that home-site advantages are context dependent and erode under rapid climate change (Alberto et al., 2013; Hereford, 2009; Leimu & Fischer, 2008; J. H. Pedlar et al., 2021; Rehfeldt et al., 2002).

By 2100, mixed provenances planting sustained approximately 2.5 times larger presence areas than locals under equal effort. Introduced provenances complemented rather than replaced locals, consistent with functional complementarity and portfolio-diversity effects (Aitken & Bemmels, 2016; Breed et al., 2019; Bucharova et al., 2019; Fady et al., 2016; Kremer et al., 2012; J. H. Pedlar et al., 2021). Recent operational trials similarly demonstrate that blending local and warm-adapted sources increases seedling establishment and drought survival (De Kort et al., 2014). This complementarity parallels experimental findings that mixtures of stress-tolerant and stress-intolerant ecotypes maximize performance under fluctuating stress (Nemer et al., 2023). Together, these results illustrate a portfolio effect akin to the assisted gene flow rationale: combining locally adapted and pre-adapted provenances enhances persistence under variable and rapidly changing climates. However, such benefits must be weighed against genetic uncertainties, including the potential for outbreeding depression and disruption of locally co-adapted gene complexes when divergent lineages interbreed (Aitken & Bemmels, 2016; Prober et al., 2015). Although our modelling framework focuses on climate matching and does not simulate genetic risks explicitly, these considerations remain important for operational deployment and highlight the need for monitoring genetic outcomes in assisted-dispersal programmes.

Spatial and altitudinal reorganization of seed exchanges

Assisted dispersal reorganized seed exchanges in a multi-directional rather than purely south-to-north pattern. Seed transfers followed climatic matching rather than geographic distance, producing a structured redistribution of origins across both horizontal and vertical gradients (Kapeller et al., 2012). Warm-oceanic Atlantic provenances (Prov 3) were consistently selected

in low-elevation warm sites, including lowland portions of the Massif Central and the Vosges-Alsace-Champagne region (Table 2). In contrast, mid- and high-elevation areas, the Vosges uplands, Alps, Jura, Massif Central uplands and Pyrenees, favoured locally adapted or climate-analogous continental and Alpine provenances (Prov 2, 4, 5, 6), reflecting cooler and more humid conditions in these mountain belts (Table 2).

Warm-oceanic provenances from the Atlantic margin (Prov 1, Prov 3) were consistently selected in low-elevation sites across central and north-western France, including lowland portions of the Massif Central (≈ 400-1100 m) and the Vosges-Alsace-Champagne region. In contrast, mid- and high-elevation areas, the Vosges uplands, Alps, Jura, Massif Central uplands, and Pyrenees, favored locally adapted or climate-analogous continental and Alpine provenances (Prov op 2, Prov 4, Prov 5, Prov 6), reflecting the cooler and more humid conditions in these mountain belts. This vertical sorting produced altitudinally stratified mixtures, with Atlantic donors dominating lowlands while continental, Alpine, and local provenances prevailed above ≈ 1100 m.

These qualitative patterns were statistically supported by our environmental analyses: provenance identity significantly predicted elevation, hottest-month and coldest-month temperatures, and dry-season precipitation (all $p < 0.0001$; Table 2). Provenance 3 was planted in the warmest and driest lowlands (highest TMXH and lowest PRDR), whereas provenances 2, 4, 5 and 6 dominated cooler, wetter uplands. Furthermore, our results mirror empirical provenance-transfer findings showing that forest-tree performance aligns with temperature-moisture regimes rather than latitude per se (Kapeller et al., 2012). They also correspond to physiological limits described for mountain treelines, where temperature thresholds govern establishment and survival, making high-elevation belts natural microclimatic refugia for trees (Körner, 2012). Similar multi-directional and altitude-structured seed flows have been reported in other temperate and boreal trees (Aitken & Bemmels, 2016; Aitken & Whitlock, 2013; Fady et al., 2016; Kapeller et al., 2012; Kremer et al., 2012; Prober et al., 2015; Serra-Diaz et al., 2016). Together, these results show that assisted dispersal should not be guided by a simple uniform poleward shift but a complex, multi-directional and altitudinally stratified redistribution of seed sources.

Limitations and assumptions of the modeling framework

Our simulations rely on SDM-derived suitability as a proxy for climate-dependent demographic rates in *simRShift* (mortality, recruitment, and establishment). Although SDMs do not explicitly model physiological process, growing empirical evidence shows that SDM probabilities correlate well with observed patterns of drought-induced mortality, regeneration failures, and demographic responses to warming in European forests (Elvira et al., 2021; Margalef-Marrase et al., 2020; Perez-Navarro et al., 2021; Thuiller et al., 2019; Urban et al., 2016). The 10-year time step balances the temporal scale of tree demographic processes with the spatial scale (1 km) of the environmental data. For *Quercus petraea*, finer demographic data, such as provenance-specific mortality curves, drought thresholds, or dispersal kernels, would further refine predictions, but are currently unavailable at national scale. Despite these limitations, coupling SDMs with dynamic simulations provides a transparent, spatially explicit, and operationally realistic way to assess the potential outcomes of assisted dispersal strategies under future climates.

We also acknowledge that our simulations do not explicitly represent interspecific competition. Both SDM projections and *simRShift* dynamics assume that *Q. petraea* responses are independent of competitors, whereas in reality, recruitment, growth, and microsite availability are strongly shaped by interactions with co-occurring tree and understory species. Incorporating competitive dynamics could modify persistence trajectories, especially in densely populated lowland forests. Likewise, planting effort in practice is shared among multiple species, meaning that large-scale investment in *Q. petraea* may reduce the capacity to assist other climate-sensitive taxa. Our estimates therefore represent the potential outcomes under dedicated planting effort, rather than the full multispecies prioritization faced by forest managers.

The need for adaptive climate-informed assisted dispersal of tree species

Our study operationalizes assisted dispersal and assisted gene flow concepts in a way that is tractable for management, by working within fixed forest seed zones used by national agencies and French National Forest Inventory (NFI). Rather than replacing zoning with complex continuous rules, we embed climate-explicit decision-making inside the forest seed zones framework: donors are chosen to match projected climate at recipient sites while respecting administrative units and likely nursery supply chains. This reconciles two needs highlighted in the literature, climate realism and operational simplicity (Alberto et al., 2013; Prober et al., 2015). The finding that some seed zones (e.g., Alps/Jura) remain self-sourced while others (e.g., Massif

Central, NE lowlands, NW oceanic) rely on targeted imports provides zone-specific guidance that foresters can implement without overhauling existing regulations.

The species' future distribution will likely depend on a dual strategy: conserving local lineages in topographic refugia and integrating climate-matched ecotypes elsewhere. Rather than replacing traditional zoning, climate-explicit provenance choice operationalizes assisted gene flow within existing national policy. This approach provides a scalable pathway for adapting European adaptation and mitigation programs to an accelerating climate change.

AUTHOR CONTRIBUTIONS

D.N. conceived and designed the study, developed the analytical workflow, and performed all simulations and data analyses. D.N. wrote the first complete draft of the manuscript

J.M.S.-D. contributed to conceptual development, supervised the research, and assisted in the interpretation of results.

L.C., M.M., M.B., and R.B. contributed to manuscript revisions and provided critical feedback on writing.

R.B. developed the original *simRShift* model (Bertrand et al., 2012) and advised on its implementation and validation.

All authors reviewed and approved the final version of the manuscript.

ACKNOWLEDGEMENTS

We thank the French National Institute of Geographic and Forest Information for making NFI data openly available, as well as every contributor of this database. DN, LC, MM, MB AND JMSD were funded by the young researchers program of the Agence National de la Recherche ANR-21-CE32-0003. JMSD acknowledges further support from the program RYC2022-035668-I, funded by MCIU/AEI/10.13039/501100011033 and FSE+. RB's work was supported by the TULIP Laboratory of Excellence (ANR-10-LABX-41),

by the Agence Nationale de la Recherche (ANR-22-CPJ2-0037-01 funding the FREEvol CPJ project; ANR-24-PEFO-0003 funding the MONITOR project of the PEPR Forestt).

DATA AND CODE AVAILABILITY

Forest inventory data used in this study are available from the French National Forest Inventory (NFI) upon request (https://inventaire-forestier.ign.fr). Climate data (CHELSA) are publicly available at https://chelsa-climate.org.

Custom R scripts used for preprocessing, SDM calibration, and simulation analyses were developed using the TuneSDM package (Nemer, in prep, https://nemerdavid.github.io/TuneSDM-docs/), which is currently under development and not yet publicly released. Due to dependencies on internal functions of TuneSDM and the *simRShift* model (Bertrand et al., 2012), which is not openly available, the full workflow cannot be directly shared.

References

Aalto, J., Karjalainen, O., Hjort, J., & Luoto, M. (2018). Statistical Forecasting of Current and Future Circum-Arctic Ground Temperatures and Active Layer Thickness. *Geophysical Research Letters*, *45*(10), 4889–4898. https://doi.org/10.1029/2018GL078007

Aalto, J., Maeda, E. E., Heiskanen, J., Aalto, E. K., & Pellikka, P. K. E. (2022). Strong influence of trees outside forest in regulating microclimate of intensively modified Afromontane landscapes. *Biogeosciences*, *19*(17), 4227–4247. https://doi.org/10.5194/bg-19-4227-2022

Aitken, S. N., & Bemmels, J. B. (2016). Time to get moving: Assisted gene flow of forest trees. *Evolutionary Applications*, *9*(1), 271–290. https://doi.org/10.1111/eva.12293

Aitken, S. N., & Whitlock, M. C. (2013). Assisted Gene Flow to Facilitate Local Adaptation to Climate Change. *Annual Review of Ecology, Evolution, and Systematics*, *44*(Volume 44, 2013), 367–388. https://doi.org/10.1146/annurev-ecolsys-110512-135747

Alberto, F. J., Aitken, S. N., Alía, R., González-Martínez, S. C., Hänninen, H., Kremer, A., Lefèvre, F., Lenormand, T., Yeaman, S., Whetten, R., & Savolainen, O. (2013). Potential for evolutionary responses to climate change—Evidence from tree populations. *Global Change Biology*, *19*(6), 1645–1661. https://doi.org/10.1111/gcb.12181

Alfaro, R. I., Fady, B., Vendramin, G. G., Dawson, I. K., Fleming, R. A., Sáenz-Romero, C., Lindig-Cisneros, R. A., Murdock, T., Vinceti, B., Navarro, C. M., Skrøppa, T., Baldinelli, G., El-Kassaby, Y. A., & Loo, J. (2014). The role of forest genetic resources in responding to biotic and abiotic factors in the context of anthropogenic climate change. *Forest Ecology and Management*, *333*, 76–87. https://doi.org/10.1016/j.foreco.2014.04.006

Allen, C. D., Macalady, A. K., Chenchouni, H., Bachelet, D., McDowell, N., Vennetier, M., Kitzberger, T., Rigling, A., Breshears, D. D., Hogg, E. H. (Ted), Gonzalez, P., Fensham, R., Zhang, Z., Castro, J., Demidova, N., Lim, J.-H., Allard, G., Running, S. W., Semerci, A., & Cobb, N. (2010). A global overview of drought and heat-induced tree mortality reveals emerging climate change risks for forests. *Forest Ecology and Management*, *259*(4), 660–684. https://doi.org/10.1016/j.foreco.2009.09.001

668 Anderegg, W. R. L., Trugman, A. T., Badgley, G., Anderson, C. M., Bartuska, A., Ciais, P.,
669 Cullenward, D., Field, C. B., Freeman, J., Goetz, S. J., Hicke, J. A., Huntzinger, D.,
670 Jackson, R. B., Nickerson, J., Pacala, S., & Randerson, J. T. (2020). Climate-driven risks
671 to the climate mitigation potential of forests. *Science*, *368*(6497), eaaz7005.
672 https://doi.org/10.1126/science.aaz7005

673 Araújo, M. B., & New, M. (2007). Ensemble forecasting of species distributions. *Trends in Ecology*
674 *& Evolution*, *22*(1), 42–47. https://doi.org/10.1016/j.tree.2006.09.010

675 Beaudoin, A., Bernier, P. Y., Villemaire, P., Guindon, L., & Guo, X. J. (2018). Tracking forest
676 attributes across Canada between 2001 and 2011 using a k nearest neighbors mapping
677 approach applied to MODIS imagery. *Canadian Journal of Forest Research*, *48*(1), 85–
678 93. https://doi.org/10.1139/cjfr-2017-0184

679 Becker, M., & Lévy, G. (1982). Le dépérissement du chêne en forêt de Tronçais Les causes
680 écologiques. *Annales Des Sciences Forestières*, *39*(4), 439–444.

681 Benito Garzón, M., Robson, T. M., & Hampe, A. (2019). ΔTraitSDMs: Species distribution models
682 that account for local adaptation and phenotypic plasticity. *New Phytologist*, *222*(4), 1757–
683 1765. https://doi.org/10.1111/nph.15716

684 Bertrand, R., Lenoir, J., Piedallu, C., Riofrío-Dillon, G., de Ruffray, P., Vidal, C., Pierrat, J.-C., &
685 Gégout, J.-C. (2011). Changes in plant community composition lag behind climate
686 warming in lowland forests. *Nature*, *479*(7374), 517–520.
687 https://doi.org/10.1038/nature10548

688 Bertrand, R., Perez, V., & Gégout, J. (2012). Disregarding the edaphic dimension in species
689 distribution models leads to the omission of crucial spatial information under climate
690 change: The case of *Q uercus pubescens* in F rance. *Global Change Biology*, *18*(8),
691 2648–2660. https://doi.org/10.1111/j.1365-2486.2012.02679.x

692 Boonman, C. C. F., Serra-Diaz, J. M., Hoeks, S., Guo, W.-Y., Enquist, B. J., Maitner, B., Malhi,
693 Y., Merow, C., Buitenwerf, R., & Svenning, J.-C. (2024). More than 17,000 tree species
694 are at risk from rapid global change. *Nature Communications*, *15*(1), 166.
695 https://doi.org/10.1038/s41467-023-44321-9

696 Breed, M. F., Harrison, P. A., Blyth, C., Byrne, M., Gaget, V., Gellie, N. J. C., Groom, S. V. C.,
697 Hodgson, R., Mills, J. G., Prowse, T. A. A., Steane, D. A., & Mohr, J. J. (2019). The
698 potential of genomics for restoring ecosystems and biodiversity. *Nature Reviews Genetics*,
699 *20*(10), 615–628. https://doi.org/10.1038/s41576-019-0152-0

700 Breiman, L. (2001). Random Forests. *Machine Learning*, *45*(1), 5–32.
701 https://doi.org/10.1023/A:1010933404324

702 Broadhurst, L. M., Lowe, A., Coates, D. J., Cunningham, S. A., McDonald, M., Vesk, P. A., &
703 Yates, C. (2008). Seed supply for broadscale restoration: Maximizing evolutionary
704 potential. *Evolutionary Applications*, *1*(4), 587–597. https://doi.org/10.1111/j.1752-
705 4571.2008.00045.x

706 Bucharova, A., Bossdorf, O., Hölzel, N., Kollmann, J., Prasse, R., & Durka, W. (2019). Mix and
707 match: Regional admixture provenancing strikes a balance among different seed-sourcing
708 strategies for ecological restoration. *Conservation Genetics*, *20*(1), 7–17.
709 https://doi.org/10.1007/s10592-018-1067-6

710 Cheaib, A., Badeau, V., Boe, J., Chuine, I., Delire, C., Dufrêne, E., cois, C., & Gritti, E. (2011).
711 Climate change impacts on tree ranges: Model inter-comparison facilitates understanding
712 and quantification of uncertainty. *Proceedings of the National Academy of Sciences of the*
713 *United States of America*, *To be submitted*.

714 Chen, T., & Guestrin, C. (2016). XGBoost: A Scalable Tree Boosting System. *Proceedings of the*
715 *22nd ACM SIGKDD International Conference on Knowledge Discovery and Data Mining*,
716 785–794. https://doi.org/10.1145/2939672.2939785

717 Clark, J. S., Beckage, B., Camill, P., Cleveland, B., HilleRisLambers, J., Lichter, J., McLachlan,
718 J., Mohan, J., & Wyckoff, P. (1999). Interpreting recruitment limitation in forests. *American*
719 *Journal of Botany*, *86*(1), 1–16. https://doi.org/10.2307/2656950

720 Coudun, C., Gégout, J., Piedallu, C., & Rameau, J. (2006). Soil nutritional factors improve models
721 of plant species distribution: An illustration with *Acer campestre* (L.) in France. *Journal of*
722 *Biogeography*, *33*(10), 1750–1763. https://doi.org/10.1111/j.1365-2699.2005.01443.x

723 De Kort, H., Vandepitte, K., Bruun, H. H., Closset-Kopp, D., Honnay, O., & Mergeay, J. (2014).
724 Landscape genomics and a common garden trial reveal adaptive differentiation to

725 temperature across Europe in the tree species Alnus glutinosa. *Molecular Ecology*, *23*(19),
726 4709–4721. https://doi.org/10.1111/mec.12813

727 Dobrowski, S. Z. (2011). A climatic basis for microrefugia: The influence of terrain on climate.
728 *Global Change Biology*, *17*(2), 1022–1035. https://doi.org/10.1111/j.1365-
729 2486.2010.02263.x

730 Ducousso, A., & Bordacs, S. (2003). *Quercus robur/Quercus petraea*.
731 https://www.euforgen.org/fileadmin//templates/euforgen.org/upload/Publications/Technic
732 al_guidelines/Technical_guidelines_Quercus_robur-petraea.pdf

733 Elith, J., & Leathwick, J. R. (2009). Species Distribution Models: Ecological Explanation and
734 Prediction Across Space and Time. *Annual Review of Ecology, Evolution, and*
735 *Systematics*, *40*(Volume 40, 2009), 677–697.
736 https://doi.org/10.1146/annurev.ecolsys.110308.120159

737 Elvira, N. J., Lloret, F., Jaime, L., Margalef-Marrase, J., Pérez Navarro, M. Á., & Batllori, E. (2021).
738 Species climatic niche explains post-fire regeneration of Aleppo pine (*Pinus halepensis*
739 Mill.) under compounded effects of fire and drought in east Spain. *Science of The Total*
740 *Environment*, *798*, 149308. https://doi.org/10.1016/j.scitotenv.2021.149308

741 Fady, B., Aravanopoulos, F. A., Alizoti, P., Mátyás, C., von Wühlisch, G., Westergren, M., Belletti,
742 P., Cvjetkovic, B., Ducci, F., Huber, G., Kelleher, C. T., Khaldi, A., Kharrat, M. B. D.,
743 Kraigher, H., Kramer, K., Mühlethaler, U., Peric, S., Perry, A., Rousi, M., … Zlatanov, T.
744 (2016). Evolution-based approach needed for the conservation and silviculture of
745 peripheral forest tree populations. *Forest Ecology and Management*, *375*, 66–75.
746 https://doi.org/10.1016/j.foreco.2016.05.015

747 Franklin, J. (2010). *Mapping Species Distributions: Spatial Inference and Prediction*. Cambridge
748 University Press. https://doi.org/10.1017/CBO9780511810602

749 Guisan, A., Lehmann, A., Ferrier, S., Austin, M., Overton, J. Mc. C., Aspinall, R., & Hastie, T.
750 (2006). Making better biogeographical predictions of species' distributions. *Journal of*
751 *Applied Ecology*, *43*(3), 386–392. https://doi.org/10.1111/j.1365-2664.2006.01164.x

752 Guitton, J. L. (1998). *Annales 1996, Département Gestion des Territoires au Cemagref* (p. 145).
753 Cemagref Editions. https://hal.inrae.fr/hal-02577243

754 Guo, W.-Y., Serra-Diaz, J. M., Eiserhardt, W. L., Maitner, B. S., Merow, C., Violle, C., Pound, M.
755 J., Sun, M., Slik, F., Blach-Overgaard, A., Enquist, B. J., & Svenning, J.-C. (2023). Climate
756 change and land use threaten global hotspots of phylogenetic endemism for trees. *Nature*
757 *Communications*, *14*(1), 6950. https://doi.org/10.1038/s41467-023-42671-y

758 Hällfors, M. H., Aikio, S., Fronzek, S., Hellmann, J. J., Ryttäri, T., & Heikkinen, R. K. (2016).
759 Assessing the need and potential of assisted migration using species distribution models.
760 *Biological Conservation*, *196*, 60–68. https://doi.org/10.1016/j.biocon.2016.01.031

761 Hällfors, M. H., Aikio, S., & Schulman, L. E. (2017). Quantifying the need and potential of assisted
762 migration. *Biological Conservation*, *205*, 34–41.
763 https://doi.org/10.1016/j.biocon.2016.11.023

764 Hanewinkel, M., Cullmann, D. A., Schelhaas, M.-J., Nabuurs, G.-J., & Zimmermann, N. E. (2013).
765 Climate change may cause severe loss in the economic value of European forest land.
766 *Nature Climate Change*, *3*(3), 203–207. https://doi.org/10.1038/nclimate1687

767 Hereford, J. (2009). A quantitative survey of local adaptation and fitness trade-offs. *The American*
768 *Naturalist*, *173*(5), 579–588. https://doi.org/10.1086/597611

769 Hufford, K. M., & Mazer, S. J. (2003). Plant ecotypes: Genetic differentiation in the age of
770 ecological restoration. *Trends in Ecology & Evolution*, *18*(3), 147–155.
771 https://doi.org/10.1016/S0169-5347(03)00002-8

772 IGN. (2013). *Fiches descriptives des grandes régions écologiques (GRECO) et des*
773 *sylvoécorégions (SER)—INVENTAIRE FORESTIER*. https://inventaire-
774 forestier.ign.fr/?article773

775 Jensen, J. (2000). Provenance Variation in Phenotypic Traits in Quercus robur and Quercus
776 petraea in Danish Provenance Trials. *Scandinavian Journal of Forest Research*, *15*, 297–
777 308. https://doi.org/10.1080/028275800447922

778 Jump, A. S., Hunt, J. M., & Peñuelas, J. (2006). Rapid climate change-related growth decline at
779 the southern range edge of Fagus sylvatica. *Global Change Biology*, *12*(11), 2163–2174.
780 https://doi.org/10.1111/j.1365-2486.2006.01250.x

781 Kapeller, S., Lexer, M. J., Geburek, T., Hiebl, J., & Schueler, S. (2012). Intraspecific variation in
782 climate response of Norway spruce in the eastern Alpine range: Selecting appropriate
783 provenances for future climate. *Forest Ecology and Management*, *271*, 46–57.
784 https://doi.org/10.1016/j.foreco.2012.01.039

785 Karger, D. N., Conrad, O., Böhner, J., Kawohl, T., Kreft, H., Soria-Auza, R. W., Zimmermann, N.
786 E., Linder, H. P., & Kessler, M. (2017). Climatologies at high resolution for the earth's land
787 surface areas. *Scientific Data*, *4*(1), 170122. https://doi.org/10.1038/sdata.2017.122

788 Kawecki, T. J., & Ebert, D. (2004). Conceptual issues in local adaptation. *Ecology Letters*, *7*(12),
789 1225–1241. https://doi.org/10.1111/j.1461-0248.2004.00684.x

790 Körner, C. (2012). *Alpine Treelines: Functional Ecology of the Global High Elevation Tree Limits*
791 (p. 220). https://doi.org/10.1007/978-3-0348-0396-0

792 Kowarik, A., & Templ, M. (2016). Imputation with the R Package VIM. *Journal of Statistical*
793 *Software*.

794 Kremer, A., Ronce, O., Robledo-Arnuncio, J. J., Guillaume, F., Bohrer, G., Nathan, R., Bridle, J.
795 R., Gomulkiewicz, R., Klein, E. K., Ritland, K., Kuparinen, A., Gerber, S., & Schueler, S.
796 (2012a). Long-distance gene flow and adaptation of forest trees to rapid climate change.
797 *Ecology Letters*, *15*(4), 378–392. https://doi.org/10.1111/j.1461-0248.2012.01746.x

798 Kuhn, M., & Johnson, K. (2013). *Applied Predictive Modeling*. Springer New York.
799 https://doi.org/10.1007/978-1-4614-6849-3

800 Kuhn, M., & Silge, J. (2022). *Tidy Modeling with R: A Framework for Modeling in the Tidyverse*.
801 O'Reilly Media, Inc.

802 Lebourgeois, F. (1999). *(Quercus petraea Liebl. Et Quercus robur L.)*.

803 Leimu, R., & Fischer, M. (2008). A Meta-Analysis of Local Adaptation in Plants. *PLoS ONE*, *3*(12),
804 e4010. https://doi.org/10.1371/journal.pone.0004010

805 Margalef-Marrase, J., Pérez-Navarro, M. Á., & Lloret, F. (2020). Relationship between heatwave-
806 induced forest die-off and climatic suitability in multiple tree species. *Global Change*
807 *Biology*, *26*(5), 3134–3146. https://doi.org/10.1111/gcb.15042

808 Marmion, M., Parviainen, M., Luoto, M., Heikkinen, R. K., & Thuiller, W. (2009). Evaluation of
809 consensus methods in predictive species distribution modelling. *Diversity and*
810 *Distributions*, *15*(1), 59–69. https://doi.org/10.1111/j.1472-4642.2008.00491.x

811 McLachlan, J. S., Hellmann, J. J., & Schwartz, M. W. (2007). A framework for debate of assisted
812 migration in an era of climate change. *Conservation Biology: The Journal of the Society*
813 *for Conservation Biology*, *21*(2), 297–302. https://doi.org/10.1111/j.1523-
814 1739.2007.00676.x

815 Nathan, R., & Muller-Landau, H. C. (2000). Spatial patterns of seed dispersal, their determinants
816 and consequences for recruitment. *Trends in Ecology & Evolution*, *15*(7), 278–285.
817 https://doi.org/10.1016/S0169-5347(00)01874-7

818 Nemer, D., Michalet, R., Randé, H., & Delerue, F. (2023). The role of ecotypic variation for plant
819 facilitation in a metal-polluted system: Stress-intolerant target ecotypes are the best
820 beneficiaries and stress-tolerant nurse ecotypes the best benefactors. *Science of The*
821 *Total Environment*, *887*, 164134. https://doi.org/10.1016/j.scitotenv.2023.164134

822 O'Neill, B. C., Tebaldi, C., van Vuuren, D. P., Eyring, V., Friedlingstein, P., Hurtt, G., Knutti, R.,
823 Kriegler, E., Lamarque, J.-F., Lowe, J., Meehl, G. A., Moss, R., Riahi, K., & Sanderson, B.
824 M. (2016). The Scenario Model Intercomparison Project (ScenarioMIP) for CMIP6.
825 *Geoscientific Model Development*, *9*(9), 3461–3482. https://doi.org/10.5194/gmd-9-3461-
826 2016

827 Pateiro-López, B., & Rodríguez-Casal, A. (2010). Generalizing the Convex Hull of a Sample: The
828 R Package alphahull. *Journal of Statistical Software*, *34*, 1–28.
829 https://doi.org/10.18637/jss.v034.i05

830 Pedlar, J. H., McKenney, D. W., & Lu, P. (2021). Critical seed transfer distances for selected tree
831 species in eastern North America. *Journal of Ecology*, *109*(6), 2271–2283.
832 https://doi.org/10.1111/1365-2745.13605

833 Pedlar, J., McKenney, D., Aubin, I., Beardmore, T., Beaulieu, J., Iverson, L., O'Neill, G., Winder,
834 R. S., & Ste-Marie, C. (2012). Extreme climate variability should be considered in forestry
835 assisted migration: A reply. *BioScience*, *63*, 317–318.

836 Perez-Navarro, M. A., Broennimann, O., Esteve, M. A., Moya-Perez, J. M., Carreño, M. F.,
837 Guisan, A., & Lloret, F. (2021). Temporal variability is key to modelling the climatic niche.
838 *Diversity and Distributions*, *27*(3), 473–484. https://doi.org/10.1111/ddi.13207

839 Prober, S. M., Byrne, M., McLean, E. H., Steane, D. A., Potts, B. M., Vaillancourt, R. E., & Stock,
840 W. D. (2015). Climate-adjusted provenancing: A strategy for climate-resilient ecological
841 restoration. *Frontiers in Ecology and Evolution*, *3*.
842 https://doi.org/10.3389/fevo.2015.00065

843 Rehfeldt, G. E., Tchebakova, N. M., Parfenova, Y. I., Wykoff, W. R., Kuzmina, N. A., & Milyutin,
844 L. I. (2002). Intraspecific responses to climate in Pinus sylvestris. *Global Change Biology*,
845 *8*(9), 912–929. https://doi.org/10.1046/j.1365-2486.2002.00516.x

846 Rellstab, C., Zoller, S., Walthert, L., Lesur, I., Pluess, A. R., Graf, R., Bodénès, C., Sperisen, C.,
847 Kremer, A., & Gugerli, F. (2016). Signatures of local adaptation in candidate genes of oaks
848 (Quercus spp.) with respect to present and future climatic conditions. *Molecular Ecology*,
849 *25*(23), 5907–5924. https://doi.org/10.1111/mec.13889

850 Rigling, A., Bigler, C., Eilmann, B., Feldmeyer-Christe, E., Gimmi, U., Ginzler, C., Graf, U., Mayer,
851 P., Vacchiano, G., Weber, P., Wohlgemuth, T., Zweifel, R., & Dobbertin, M. (2013). Driving
852 factors of a vegetation shift from Scots pine to pubescent oak in dry Alpine forests. *Global*
853 *Change Biology*, *19*(1), 229–240. https://doi.org/10.1111/gcb.12038

854 Savolainen, O., Pyhäjärvi, T., & Knürr, T. (2007). Gene Flow and Local Adaptation in Trees.
855 *Annual Review of Ecology, Evolution, and Systematics*, *38*(Volume 38, 2007), 595–619.
856 https://doi.org/10.1146/annurev.ecolsys.38.091206.095646

857 Seidl, R., & Senf, C. (2024). Changes in planned and unplanned canopy openings are linked in
858 Europe's forests. *Nature Communications*, *15*(1), 4741. https://doi.org/10.1038/s41467-
859 024-49116-0

860 Seidl, R., Thom, D., Seibold, S., Maroschek, M., & Rammer, W. (2025). Climate change threatens
861 old-growth forests in the Northern Alps. *Environmental Research Letters*, *20*(9), 094057.
862 https://doi.org/10.1088/1748-9326/adf861

863 Senf, C., Buras, A., Zang, C. S., Rammig, A., & Seidl, R. (2020). Excess forest mortality is
864 consistently linked to drought across Europe. *Nature Communications*, *11*(1), 6200.
865 https://doi.org/10.1038/s41467-020-19924-1

866 Serra-Diaz, J. M., Borderieux, J., Maitner, B., Boonman, C. C. F., Park, D., Guo, W.-Y., Callebaut,
867 A., Enquist, B. J., Svenning, J.-C., & Merow, C. (2024). occTest: An integrated approach
868 for quality control of species occurrence data. *Global Ecology and Biogeography*, *33*(7),
869 e13847. https://doi.org/10.1111/geb.13847

870 Serra-Diaz, J. M., Franklin, J., Dillon, W. W., Syphard, A. D., Davis, F. W., & Meentemeyer, R. K.
871 (2016). Early indications of tree range shifts. *Global Ecology and Biogeography*, *25*(2),
872 164–175. https://doi.org/10.1111/geb.12396

873 Serra-Diaz, J. M., Franklin, J., Ninyerola, M., Davis, F. W., Syphard, A. D., Regan, H. M., &
874 Ikegami, M. (2014). Bioclimatic velocity: The pace of species exposure to climate change.
875 *Diversity and Distributions*, *20*(2), 169–180. https://doi.org/10.1111/ddi.12131

876 Serra-Diaz, J. M., Maxwell, C., Lucash, M. S., Scheller, R. M., Laflower, D. M., Miller, A. D.,
877 Tepley, A. J., Epstein, H. E., Anderson-Teixeira, K. J., & Thompson, J. R. (2018).
878 Disequilibrium of fire-prone forests sets the stage for a rapid decline in conifer dominance
879 during the 21st century. *Scientific Reports*, *8*(1), 6749. https://doi.org/10.1038/s41598-
880 018-24642-2

881 Ste-Marie, C., A. Nelson, E., Dabros, A., & Bonneau, M.-E. (2011). Assisted migration:
882 Introduction to a multifaceted concept. *The Forestry Chronicle*, *87*(06), 724–730.
883 https://doi.org/10.5558/tfc2011-089

884 Thuiller, W., Guéguen, M., Renaud, J., Karger, D. N., & Zimmermann, N. E. (2019). Uncertainty
885 in ensembles of global biodiversity scenarios. *Nature Communications*, *10*(1), 1446.
886 https://doi.org/10.1038/s41467-019-09519-w

887 Trumbore, S., Brando, P., & Hartmann, H. (2015). Forest health and global change. *Science*,
888 *349*(6250), 814–818. https://doi.org/10.1126/science.aac6759

889 Urban, M. C., Bocedi, G., Hendry, A. P., Mihoub, J.-B., Pe'er, G., Singer, A., Bridle, J. R., Crozier,
890 L. G., De Meester, L., Godsoe, W., Gonzalez, A., Hellmann, J. J., Holt, R. D., Huth, A.,
891 Johst, K., Krug, C. B., Leadley, P. W., Palmer, S. C. F., Pantel, J. H., … Travis, J. M. J.

(2016). Improving the forecast for biodiversity under climate change. *Science*, *353*(6304), aad8466. https://doi.org/10.1126/science.aad8466

Vitasse, Y., Delzon, S., Dufrêne, E., Pontailler, J.-Y., Louvet, J.-M., Kremer, A., & Michalet, R. (2009). Leaf phenology sensitivity to temperature in European trees: Do within-species populations exhibit similar responses? *Agricultural and Forest Meteorology*, *149*, 735–744. https://doi.org/10.1016/j.agrformet.2008.10.019

Williams, M. I., & Dumroese, R. K. (2013). Preparing for Climate Change: Forestry and Assisted Migration. *Journal of Forestry*, *111*(4), 287–297. https://doi.org/10.5849/jof.13-016

Xu, T., & Hutchinson, M. (2011). *ANUCLIM VERSION 6.1 USER GUIDE*.

Zurell, D., Franklin, J., König, C., Bouchet, P. J., Dormann, C. F., Elith, J., Fandos, G., Feng, X., Guillera-Arroita, G., Guisan, A., Lahoz-Monfort, J. J., Leitão, P. J., Park, D. S., Peterson, A. T., Rapacciuolo, G., Schmatz, D. R., Schröder, B., Serra-Diaz, J. M., Thuiller, W., … Merow, C. (2020). A standard protocol for reporting species distribution models. *Ecography*, *43*(9), 1261–1277. https://doi.org/10.1111/ecog.04960

Tables

Table 1. Estimated marginal means (± SE) of preserved area and planting efficiency across years (2030-2100), derived from linear mixed-effects models (LMMs) with planting effort as a fixed effect and year as a random intercept. Preserved area corresponds to total occupied area (×10³ ha), and efficiency is expressed as the gain in occupied cells relative to the no-planting baseline per 1,000 planted cells (%). Different letters within each column indicate significant pairwise differences among planting efforts (Tukey-adjusted $p < 0.05$). Overall effects of planting effort were highly significant for both preserved area and efficiency ($p < 0.0001$).

Planting effort	Preserved area (×10³ ha) ± SE	Tukey group	Efficiency (%) ± SE	Tukey group
5%	548 ± 214	D	170.0 ± 47.4	C
10%	624 ± 204	D	101.0 ± 22.4	CB
25%	813 ± 183	C	54.8 ± 8.51	AB
50%	1047 ± 165	B	36.5 ± 4.76	AB
100%	1386 ± 160	A	24.4 ± 2.87	A

Table 2. Environmental characteristics of planting locations for each provenance, based on linear mixed-effects models (LMMs). Values represent estimated marginal means (± SE) of elevation, mean annual maximum temperature of the hottest month (TMXH), mean annual minimum temperature of the coldest month (TMNC), and total precipitation of the driest quarter (PRDR). Provenance was treated as a fixed effect and planting year as a random intercept. Different letters within each column indicate significant pairwise differences (Tukey-adjusted $p < 0.05$). Overall provenance effects were highly significant for all variables ($p < 0.0001$).

Provenance	Elevation (m) ± SE	Tukey group	TMXH (°C) ± SE	Tukey group	TMNC (°C) ± SE	Tukey group	PRDR (mm) ± SE	Tukey group
2-Northeastern continental	942 ± 33.1	D	24.9 ± 0.28	B	–3.31 ± 0.27	D	65.6 ± 3.86	B
3-Southwestern Atlantic	226 ± 38	E	27.0 ± 0.29	A	0.16 ± 0.29	E	35.9 ± 3.96	E
4-Massif Central	1102 ± 36	B	24.6 ± 0.27	D	–2.83 ± 0.28	C	60.8 ± 3.90	D
5-Alpine/Jura	1046 ± 35	C	25.9 ± 0.28	B	–5.44 ± 0.27	A	93.8 ± 3.77	A
6-Pyrenean	1351 ± 38	A	23.4 ± 0.28	E	–4.00 ± 0.29	B	62.7 ± 3.94	C

Figure captions

Figure 1. Current distribution of *Quercus petraea* and projected climatic changes across French seed zones.
(A) Present-day distribution of *Q. petraea* and the location of the six provenance clusters used to define seed origins.
(B) Projected mean changes in key temperature and precipitation variables between 2020-2030 and 2090-2100 under the MRI-SSP585 scenario. Values represent mean change per seed zone (Δ = 2090-2100 minus 2020-2030). Numbers indicate provenance identities: 1 = Northwestern Atlantic, 2 = Northeastern continental, 3 = Southwestern Atlantic, 4 = Massif Central, 5 = Alpine-Jura, 6 = Pyrenean.

Figure 2. Effects of seed sourcing strategy on the range persistence of *Quercus petraea* through the 21st century.
(A) Maps of predicted species presence from 2030 to 2100 simulated with *simRShift* under three scenarios: no planting, local provenances only, and mixed provenances, assuming a 5% planting effort (years shown: 2030, 2080, and 2100).
(B) Temporal trajectories of total occupied area (10^3 ha) from 2030 to 2100 for each scenario (years shown: 2050 to 2100).

Figure 3. Spatial and temporal dynamics of planted provenance origins under the 5% planting scenario**.**
(A) Temporal evolution of planted origins for Local provenances (top row) and Mixed provenances (bottom row) strategies from 2030 to 2090.
(B) Mean contribution of each provenance to planting within seed zones, expressed as the average proportion of planted cells across years (donut charts).
(C) Topography of France showing major mountain systems (Vosges, Jura, Alps, Massif Central, Pyrenees), illustrating how elevation gradients correspond to patterns of provenance allocation and persistence.
(D) Relative planting effort per seed zone, expressed as the proportion of planted cells allocated to each region across years. Colours correspond to provenance identities as in Figure 1.

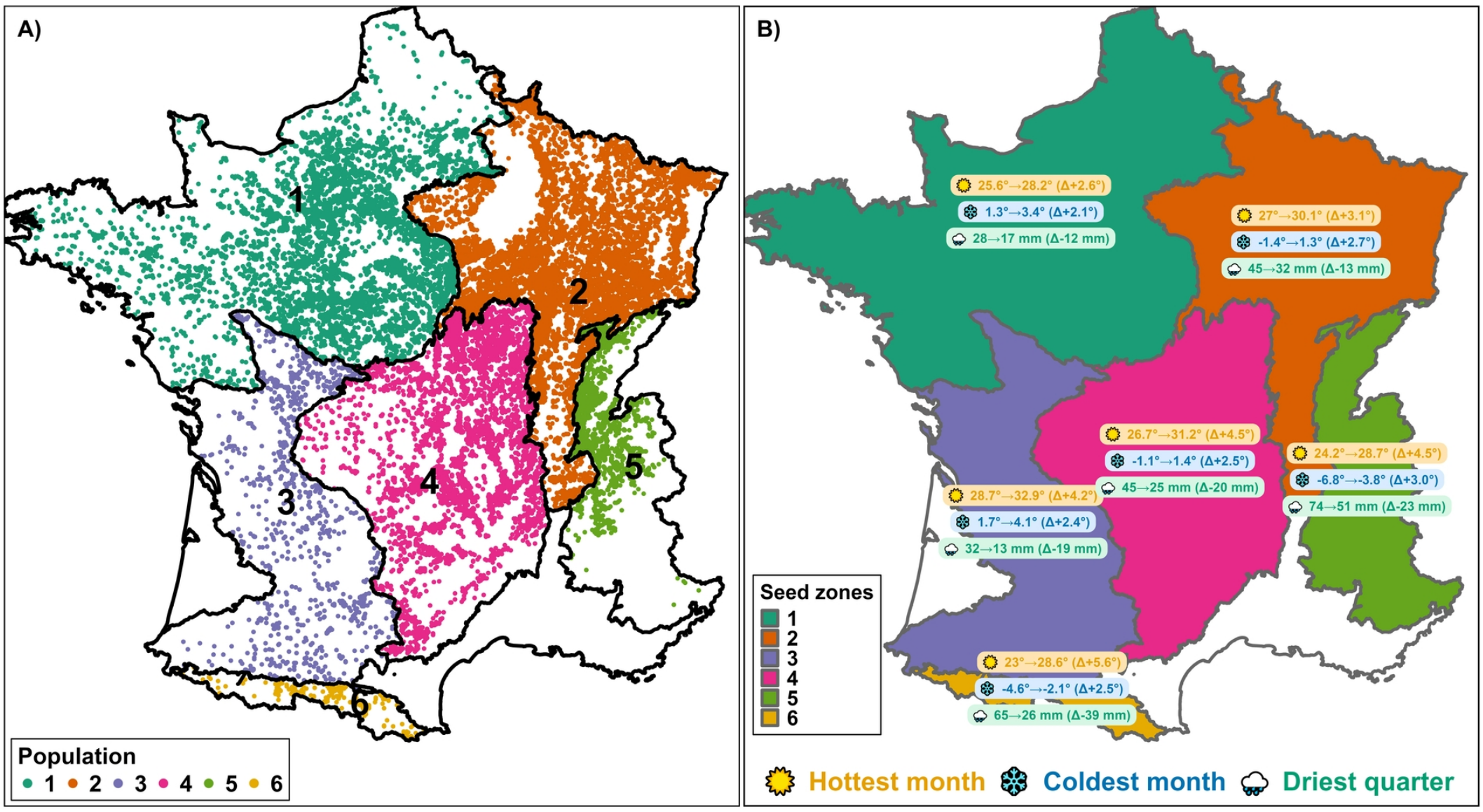
A)
1
2
3
4
5
6
Population
1 2 3 4 5 6
B)
25.6°→28.2° (Δ+2.6°)
1.3°→3.4° (Δ+2.1°)
28→17 mm (Δ-12 mm)
27°→30.1° (Δ+3.1°)
-1.4°→1.3° (Δ+2.7°)
45→32 mm (Δ-13 mm)
26.7°→31.2° (Δ+4.5°)
-1.1°→1.4° (Δ+2.5°)
45→25 mm (Δ-20 mm)
24.2°→28.7° (Δ+4.5°)
-6.8°→-3.8° (Δ+3.0°)
74→51 mm (Δ-23 mm)
28.7°→32.9° (Δ+4.2°)
1.7°→4.1° (Δ+2.4°)
32→13 mm (Δ-19 mm)
Seed zones
1
2
3
4
5
6
23°→28.6° (Δ+5.6°)
-4.6°→-2.1° (Δ+2.5°)
65→26 mm (Δ-39 mm)
Hottest month
Coldest month
Driest quarter

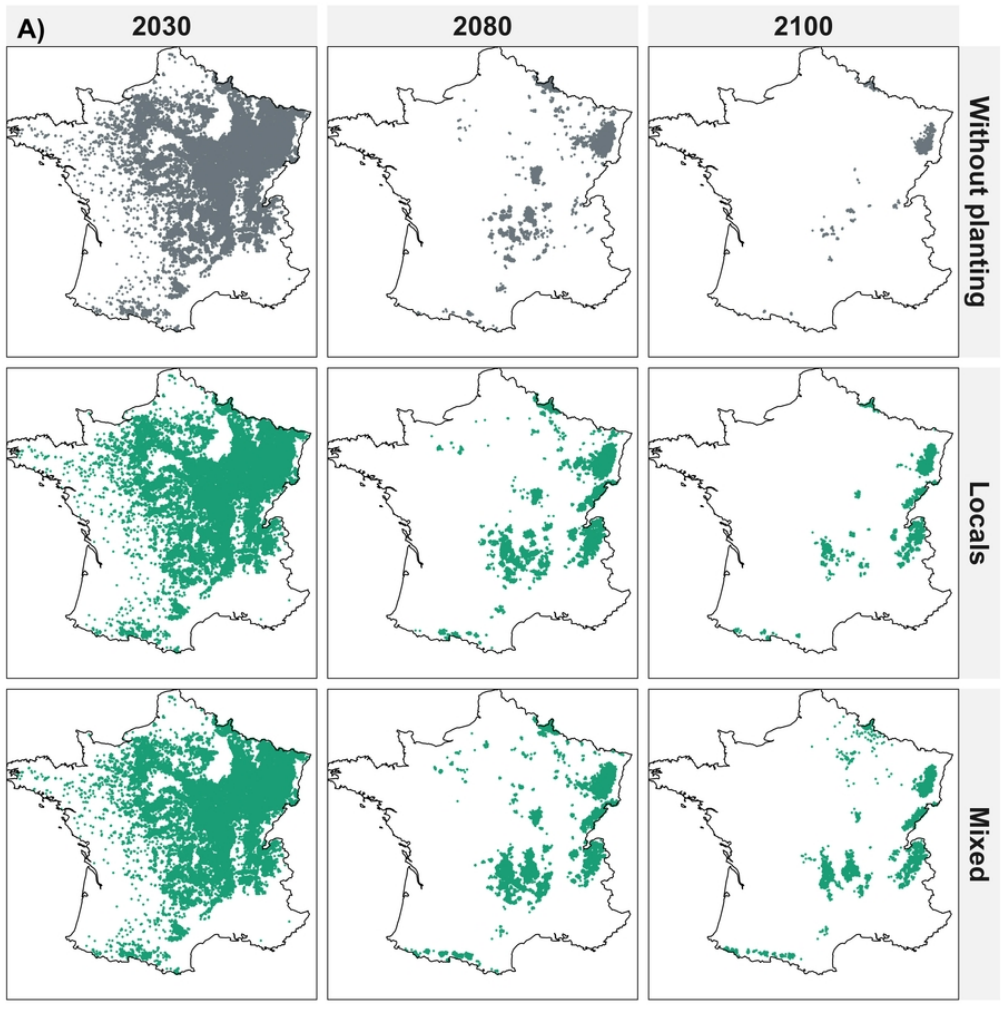
A)
2030
2080
2100
Without planting
Locals
Mixed

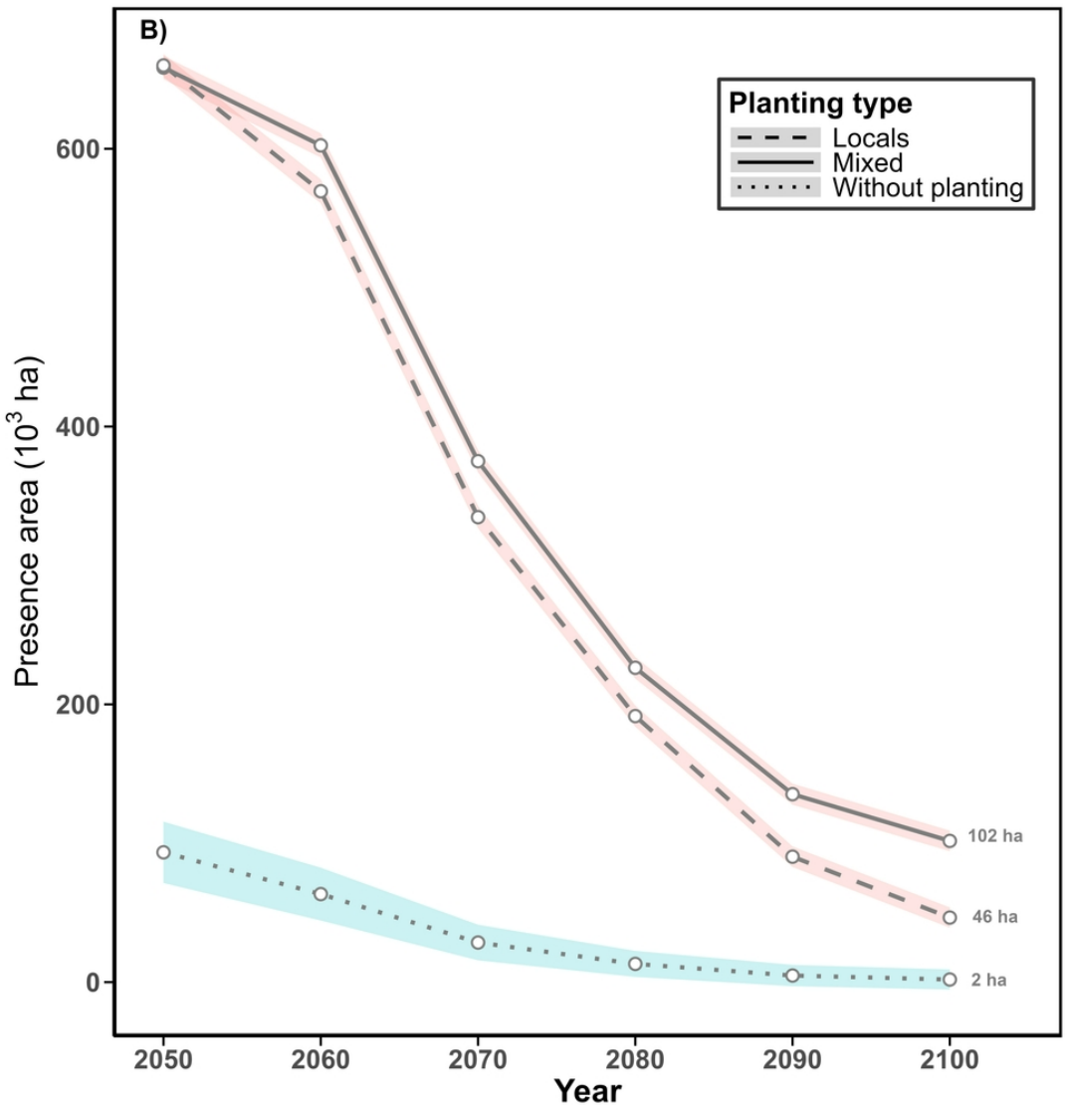
B)
Planting type
Locals
Mixed
Without planting
Presence area (10^3 ha)
600
400
200
0
102 ha
46 ha
2 ha
2050
2060
2070
2080
2090
2100
Year

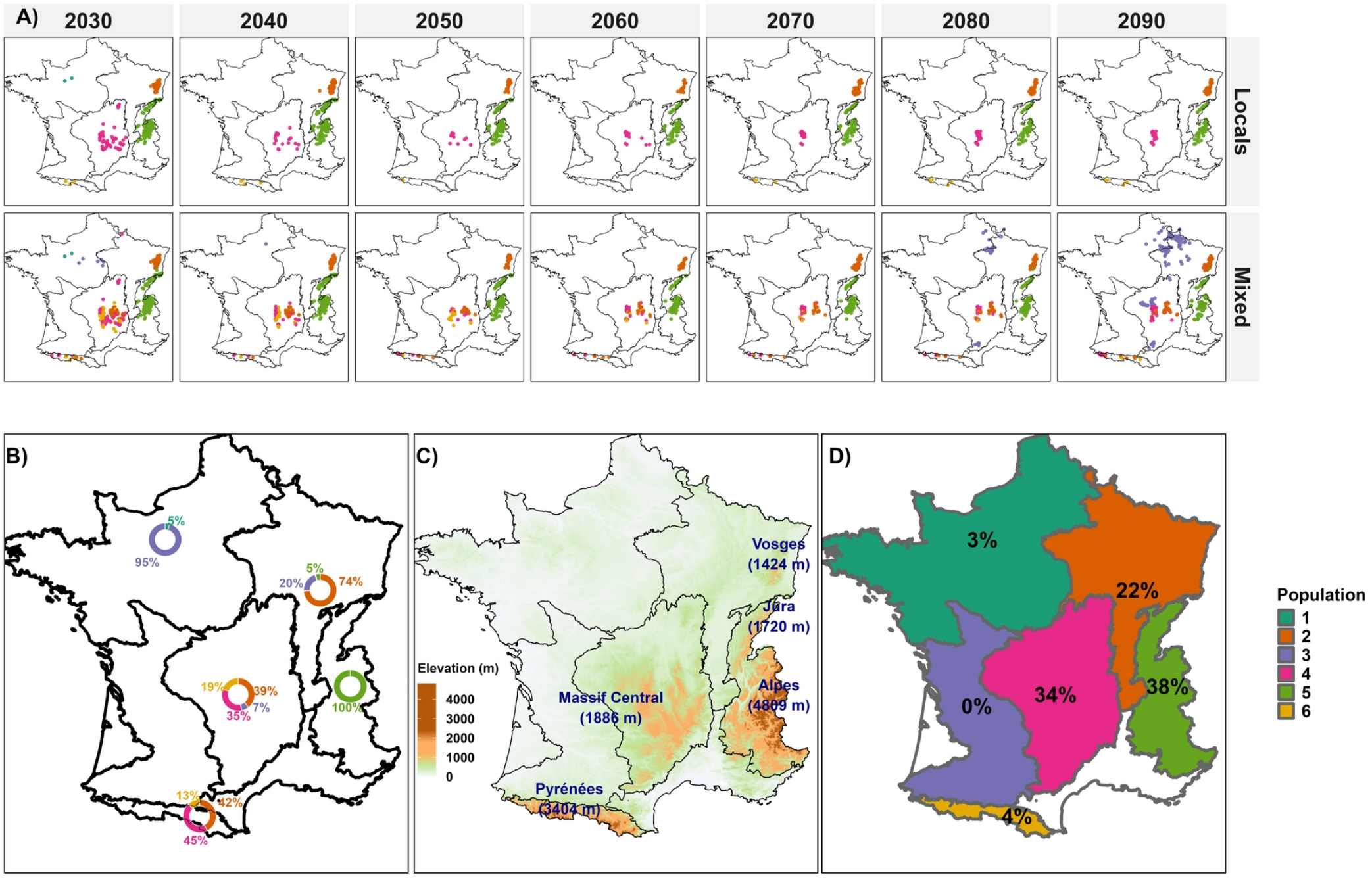
A)
2030
2040
2050
2060
2070
2080
2090
Locals
Mixed
B)
5%
95%
5%
20%
74%
19%
39%
35%
7%
100%
13%
42%
45%
C)
Vosges
(1424 m)
Jura
(1720 m)
Elevation (m)
4000
3000
2000
1000
0
Massif Central
(1886 m)
Alpes
(4809 m)
Pyrénées
(3404 m)
D)
3%
22%
0%
34%
38%
4%
Population
1
2
3
4
5
6

Global Circulation model selection:

To identify the most reliable CMIP6 models over metropolitan France, the performance of four GCMs (MRI-ESM2-0, IPSL-CM6A-LR, GFDL-ESM4, and MPI-ESM1-2-HR) was assessed against monthly observations from Météo-France weather stations for the period 2015-2023.

Model performance was evaluated using three metrics: Root Mean Square Error (RMSE), which measures the average deviation from observations; Bias, which quantifies systematic over- or underestimation. Each metric was calculated for four variables: mean temperature (tas), maximum temperature (tasmax), minimum temperature (tasmin), and precipitation (pr) under two emission scenarios (SSP3-7.0 and SSP5-8.5).

The evaluation used 97,020 precipitation records from 914 stations, and a total of 83,196 temperature records, consisting of 24,336 mean-temperature records from 227 stations, 28,908 minimum-temperature records from 270 stations, and 29,952 maximum-temperature records from 281 stations, covering the period 2015-2023. This extensive observational database ensures robust spatial and climatic coverage across metropolitan France. Each GCM received a rank (1-4) for every variable and emission scenario based on RMSE, with lower RMSE values indicating better performance. A weighted scoring system was then applied to derive the overall model ranking: 4 points for Rank 1, 3 points for Rank 2, 2 points for Rank 3, and 1 point for Rank 4. The total score for each GCM corresponds to the sum of these weighted ranks across all variables and scenarios.
This ranking-based approach provides an empirical yet transparent framework to identify GCMs with the best overall agreement with observed climatology, consistent with previous regional model evaluation studies (e.g., Knutti et al., 2010; McSweeney et al., 2015).

Table 1 summarizes the comparative performance of the four CMIP6 GCMs across variables and scenarios. Based on the ranking, the models MRI-ESM2-0, GFDL-ESM4, and IPSL-CM6A-LR demonstrated the lowest RMSE and bias values and were therefore retained for downscaling. The MPI-ESM1-2-HR model exhibited consistently higher RMSE values, particularly for temperature variables, and was therefore excluded from the set of models retained for downscaling.

Table 1. Performance-based ranking of four CMIP6 General Circulation Models over metropolitan France (2015–2023), evaluated using RMSE across four climate variables and two emission scenarios (SSP3-7.0 and SSP5-8.5).

Model	Rank 1	Rank 2	Rank 3	Rank 4	Total Score = 4×R1 + 3×R2 + 2×R3 + 1×R4
MRI-ESM2-0	3	4	1	0	26
GFDL-ESM4	2	3	3	0	23
IPSL-CM6A-LR	3	2	1	2	22
MPI-ESM1-2-HR	2	0	2	4	16

To complement the overall ranking presented in Table 1, Table 2 provides the detailed evaluation results for each climate variable (precipitation, mean temperature, minimum temperature, and maximum temperature) under both emission scenarios (SSP3-7.0 and SSP5-8.5). For each model, the Bias, RMSE are reported along with the corresponding

performance rank. This detailed breakdown allows a more nuanced interpretation of how each GCM performs across different components of the French climate system.

Table 2. Detailed performance metrics of CMIP6 General Circulation Models (GCMs) for precipitation and temperature variables over metropolitan France (2015–2023), including Bias, RMSE, number of stations, and ranking under SSP3-7.0 and SSP5-8.5.

Variable	Emission Scenario (SSP)	General Circulation Model (GCM)	Bias	RMSE	Rang
Precipitation	ssp370	IPSL-CM6A-LR	-3.88	36.82	1
		MRI-ESM2-0	8.78	41.52	2
		GFDL-ESM4	3.23	43.21	3
		MPI-ESM1-2-HR	12.45	49.66	4
	ssp585	GFDL-ESM4	7.5	40.32	1
		IPSL-CM6A-LR	2.94	41.82	2
		MRI-ESM2-0	4.4	43.33	3
		MPI-ESM1-2-HR	7.88	45.08	4
Mean Temperature	ssp370	MRI-ESM2-0	-0.34	3.53	1
		GFDL-ESM4	-0.22	3.74	2
		IPSL-CM6A-LR	-0.41	3.82	3
		MPI-ESM1-2-HR	-1.15	3.9	4
	ssp585	MPI-ESM1-2-HR	-0.89	3.73	1
		GFDL-ESM4	-0.62	3.8	2
		MRI-ESM2-0	-0.12	3.81	3
		IPSL-CM6A-LR	-0.59	3.82	4
		MRI-ESM2-0	0.59	1.53	1

Minimum Temperature	ssp370	IPSL-CM6A-LR	0.47	1.87	2
		MPI-ESM1-2-HR	-0.1	1.87	3
		GFDL-ESM4	0.79	2.14	4
	ssp585	MPI-ESM1-2-HR	-0.02	1.6	1
		IPSL-CM6A-LR	0.31	1.96	2
		MRI-ESM2-0	0.75	2.02	3
		GFDL-ESM4	0.42	2.08	4
Maximum Temperature	ssp370	MRI-ESM2-0	-1.48	2.37	1
		GFDL-ESM4	-1.44	2.72	2
		IPSL-CM6A-LR	-1.49	2.86	3
		MPI-ESM1-2-HR	-2.42	3.51	4
	ssp585	MRI-ESM2-0	-1.18	2.68	1
		IPSL-CM6A-LR	-1.7	2.85	2
		GFDL-ESM4	-1.85	3.06	3
		MPI-ESM1-2-HR	-2.26	3.24	4

Study on methodology in species distribution modeling

– ODMAP Protocol –

David Nemer

2025-27-02

Overview

Authorship

Contact : david.nemer@agroparistech.fr

Model objective

Model objective: Forecast and transfer

Target output: Suitable vs. unsuitable habitat

Focal Taxon

Focal Taxon: Quercus petraea

Scale of Analysis

Spatial extent: 123900, 1241900, 6049652, 7110652 (xmin, xmax, ymin, ymax)

Spatial resolution: 1000 (km)

Temporal extent: 1981-2020, 2020-2100

Boundary: natural

Biodiversity data

Observation type: French National Forest Inventory (NFI)

Response data type: presence-absence

Predictors

Predictor types: climatic

Algorithms

Modelling techniques: XGBoost, randomForest

Model averaging: Averaging/ensemble modelling

Workflow

Model workflow:

1. Presence-absence data were extracted from the French National Forest Inventory (NFI). NFI data were filtered to include only plots with valid species information by removing records with missing or incomplete species identifications.
2. Data splitting into training and test sets.
3. Model specification for RF and XGBoost.
4. Cross-validation and tuning.
5. Final model selection and fitting.
6. Making predictions on the test set and evaluating models using AUC metrics.
7. Ensemble modelling.
8. Predictions on the current & future climate

Software

Software: Software: R version 4.3.2. key packages (raster, terra sf, tidymodels)

Data

Biodiversity data

Taxon names: Quercus petraea

Ecological level: species

Data sources: French National Forest Inventory (NFI)

Data partitioning

Training data: Data splitting into training (70%) and test sets (30%)

Validation data: Cross-validation

Predictor variables

Predictor variables:

Maximum temperature of the hottest month (TMXH), Minimum temperature of the coldest month (TMNC), Precipitation of the driest quarter (PRDR), Soil pH

Data sources: CHELSA database (Karger et al., 2017)

Spatial extent: 123900, 1241900, 6049652, 7110652 (xmin, xmax, ymin, ymax)

Spatial resolution: 1 km

Coordinate reference system: lon/lat WGS 84 (EPSG:4326)

Temporal extent: 1981-2020

Transfer data

Data sources: CHELSA database (Karger et al., 2017)

Spatial extent: 123900, 1241900, 6049652, 7110652 (xmin, xmax, ymin, ymax)

Spatial resolution: 1 km

Temporal extent: 2020-2100

Models and scenarios: MRI_ESM2 (ssp585)

Model

Model settings

XGBoost: formula (pa~ TMXH + TMNC + PRDR)

randomForest: formula (pa~ TMXH + TMNC + PRDR)

Threshold selection

Threshold selection: Threshold selection: Minimum Training Presence

Assessment

Performance statistics

Performance on training data: AUC

Performance on validation data: AUC

Performance on test data: AUC

Plausibility check

Response shapes: partial response plots

Expert judgement: map display

Prediction

Prediction output

Prediction unit: Probability

Random Forest and Gradient Boosting Machine models were used to predict the distribution of the species across different time periods, including the current climate and future periods (2020-2100). For the future climate scenarios, one General Circulation Models (GCM) was utilized: MRI_ESM2 under two Shared Socioeconomic Pathways (SSPs): SSP585. To enhance the robustness of the predictions, an ensemble approach combining RF and XGBoost was applied.

We quantified site fertility using a spatially explicit index derived from dominant height, which is widely used as a dendrometric measure of site quality (site index) in even-aged forests. Site index is classically defined as the average height of dominant and codominant trees at a reference age and is considered the most widely accepted quantitative indicator of site productivity in many forest regions (Engel et al., 2023; Hanson et al., 2003).

We used national forest inventory plots as calibration data. For each plot, dominant height (Hdom, m) was computed as the mean height of dominant trees (Sharma et al., 2011). Explanatory variables included soil and site properties (available water capacity, pH, C/N ratio, slope) (Bravo-Oviedo et al., 2008), stand structure (age, relative stand density index), species identity, and climatic descriptors (mean annual temperature and precipitation).

A Random Forest model (implemented with the ranger package) was fitted to predict Hdom as a function of all environmental and stand variables.

To derive a map of soil fertility, we applied the fitted model to a 1-km grid covering the study area. For each grid cell, we extracted the soil and site variables and fixed non-edaphic covariates to standard reference conditions (pure beech stand, reference age of 100 years, median relative density, and median climate). Under these standardized stand and climate conditions, spatial variation in predicted dominant height primarily reflects differences in soil-related site quality. We then linearly rescaled Hdom between its minimum and maximum predicted values to obtain a dimensionless fertility index ranging from 0 (lowest fertility within the study area) to 1 (highest fertility)

Bravo-Oviedo, A., Tomé, M., Bravo, F., Montero, G., del Río, M., 2008. Dominant height growth equations including site attributes in the generalized algebraic difference approach. Can. J. For. Res. 38, 2348–2358. https://doi.org/10.1139/X08-077

Engel, M., Mette, T., Falk, W., Poschenrieder, W., Fridman, J., Skudnik, M., 2023. Modelling Dominant Tree Heights of Fagus sylvatica L. Using Function-on-Scalar Regression Based on Forest Inventory Data. Forests 14, 304. https://doi.org/10.3390/f14020304

Hanson, E.J., Azuma, D.L., Hiserote, B.A., 2003. Site Index Equations and Mean Annual Increment Equations for Pacific Northwest Research Station Forest Inventory and Analysis Inventories, 1985-2001.

Sharma, R.P., Brunner, A., Eid, T., Øyen, B.-H., 2011. Modelling dominant height growth from national forest inventory individual tree data with short time series and large age errors. For. Ecol. Manag. 262, 2162–2175. https://doi.org/10.1016/j.foreco.2011.07.037

Provenances	ROC-AUC	TSS
Q.petarea 1	0.94	0.75
Q.petarea 2	0.94	0.79
Q.petarea 3	0.95	0.82
Q.petarea 4	0.93	0.75
Q.petarea 5	0.98	0.93
Q.petarea 6	0.93	0.72

Table S1. Predictive performance metrics of provenance-specific species distribution models (SDMs) for *Quercus petraea* (provenances 1-6). Values correspond to ensemble mean scores combining Random Forest and XGBoost models. ROC-AUC = area under the receiver operating characteristic curve; TSS = True Skill Statistic.

Species	Maximum Dispersal Distance (meters)	Age of maturity (years)	Maximum lifespan (years)	Masting event per decade	Reference
Quercus petraea	4000	40	800	3	1) *Bonner, F.T., Karrfalt, R.P. & Nisley, R.G. 2008.* The woody plant seed manual*. USDA Forest Service, Agricultural Handbook 727, Washington, DC, 1223 pp.* 2) Vittoz, P., & Engler, R. (2007). Seed dispersal distances: A typology based on dispersal modes and plant traits. *Botanica Helvetica*, *117*(2), 109–124. https://doi.org/10.1007/s00035-007-0797-8

Table S2. Species-specific demographic and dispersal traits used as input parameters in the *simRShift* (SRS) model for *Quercus petraea*, including maximum dispersal distance, age at maturity, maximum lifespan, and frequency of masting events.

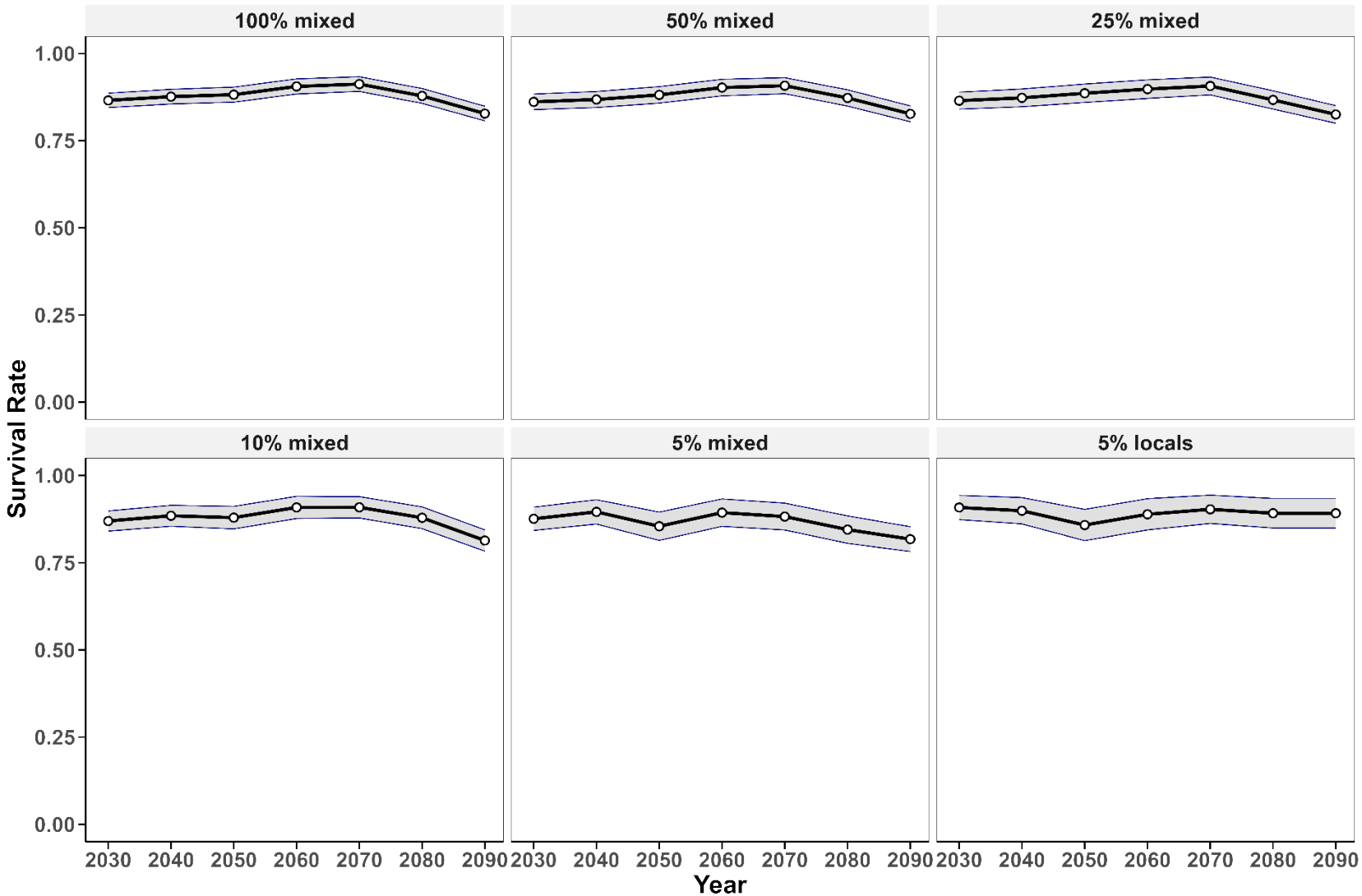

Figure S1. Effects of post-hoc survival filtering from 2030 to 2100 on survival rates (mean ± SE) across planting strategies and effort levels (e.g. 5-100% mixed, 5% local-only).

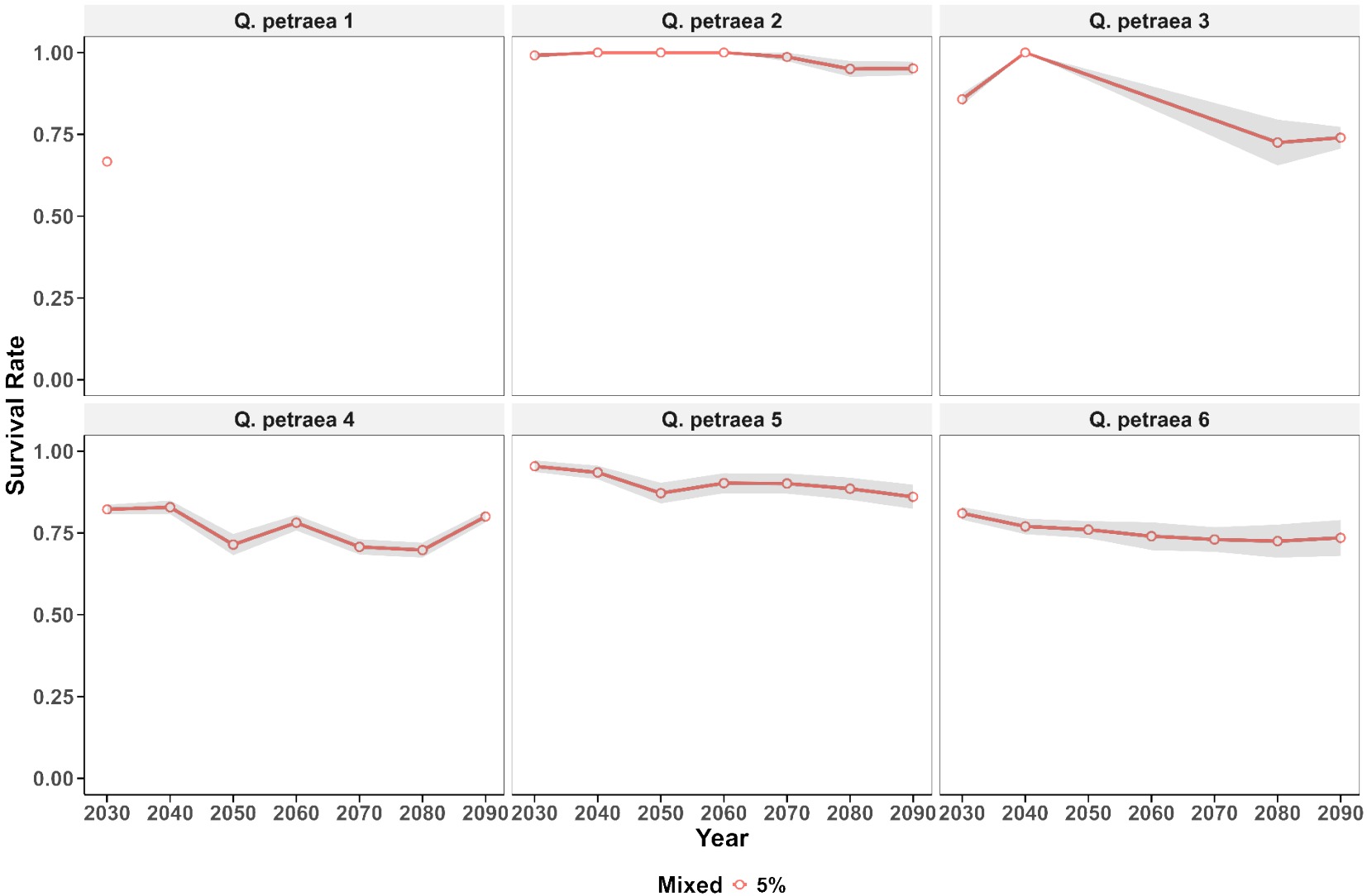
Q. petraea 1
Q. petraea 2
Q. petraea 3
Q. petraea 4
Q. petraea 5
Q. petraea 6
Survival Rate
1.00
0.75
0.50
0.25
0.00
2030
2040
2050
2060
2070
2080
2090
Year
Mixed
5%

Figure S2. Effects of post-hoc survival filtering on survival rates (mean ± SE) for each planted provenance across decades under the 5% mixed-provenance strategy. Provenance 1 was only used in 2030.

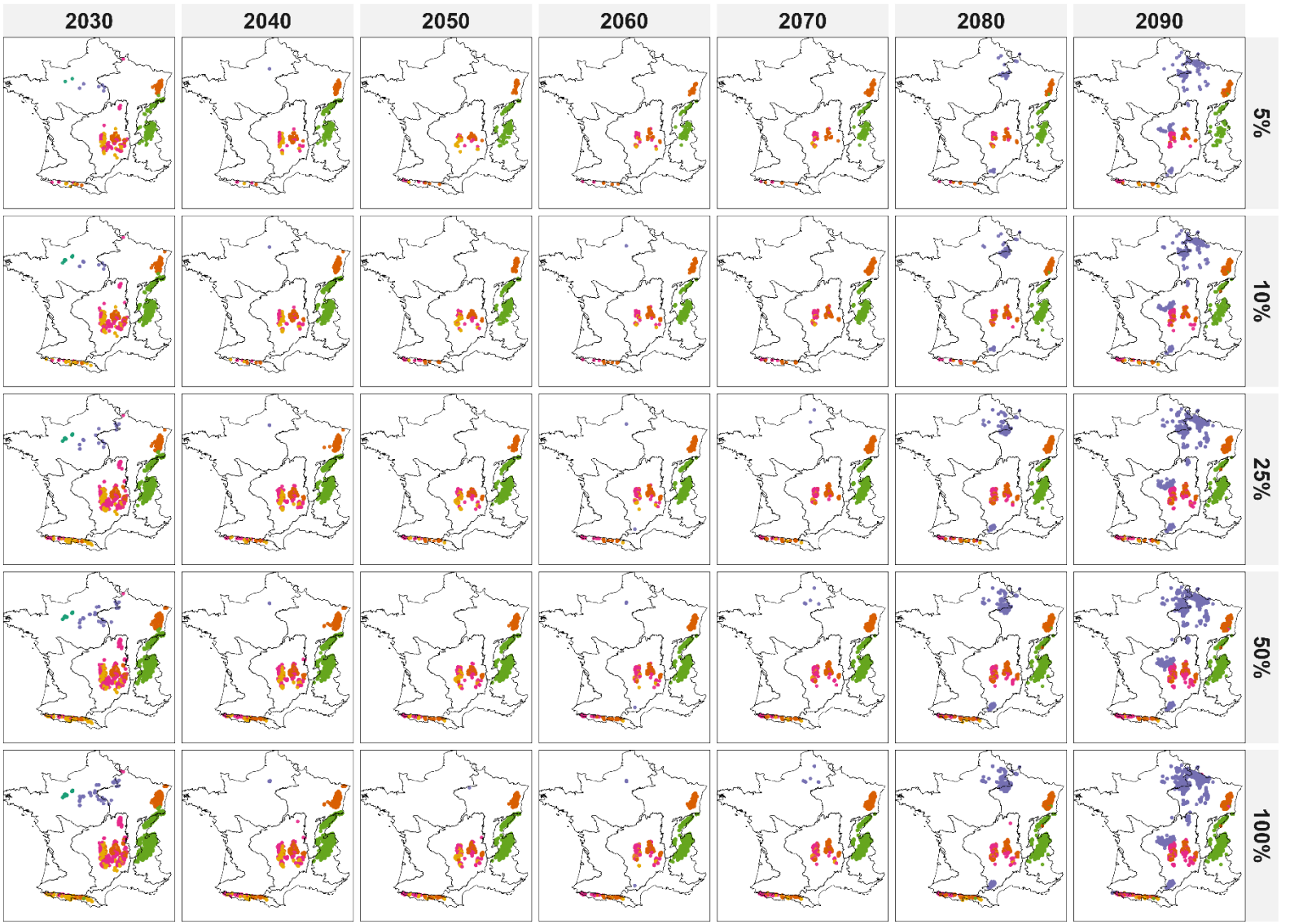

Figure S3. Spatial distribution of planted provenance origins for the mixed-provenance strategy under increasing planting efforts (5%, 10%, 25%, 50%, 100%) from 2030 to 2090.

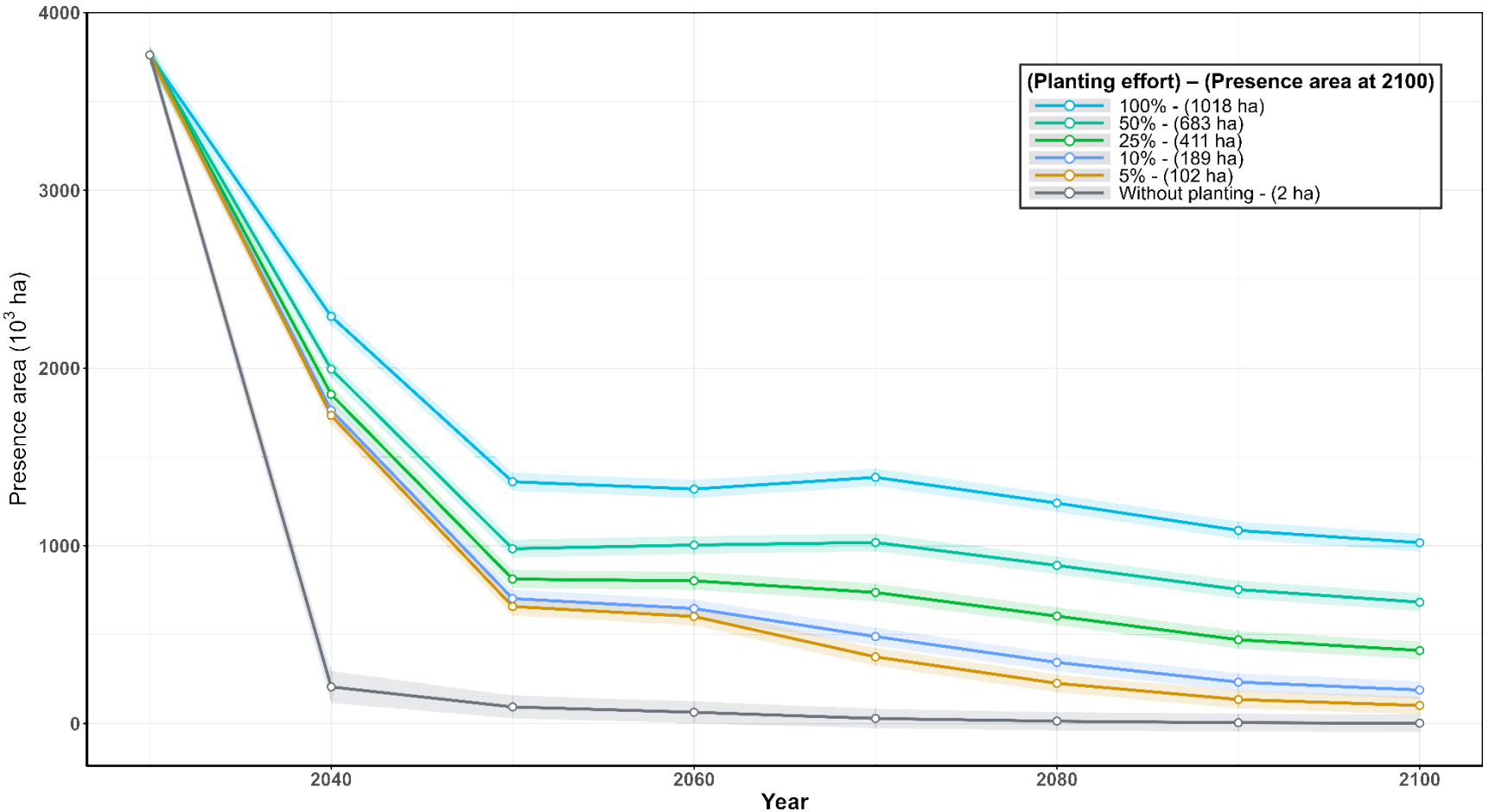

Figure S4. Temporal dynamics of total occupied area (10^3 ha) from 2030 to 2100 comparing mixed-provenance strategies across planting-effort levels (5-100%) and the no-planting baseline.

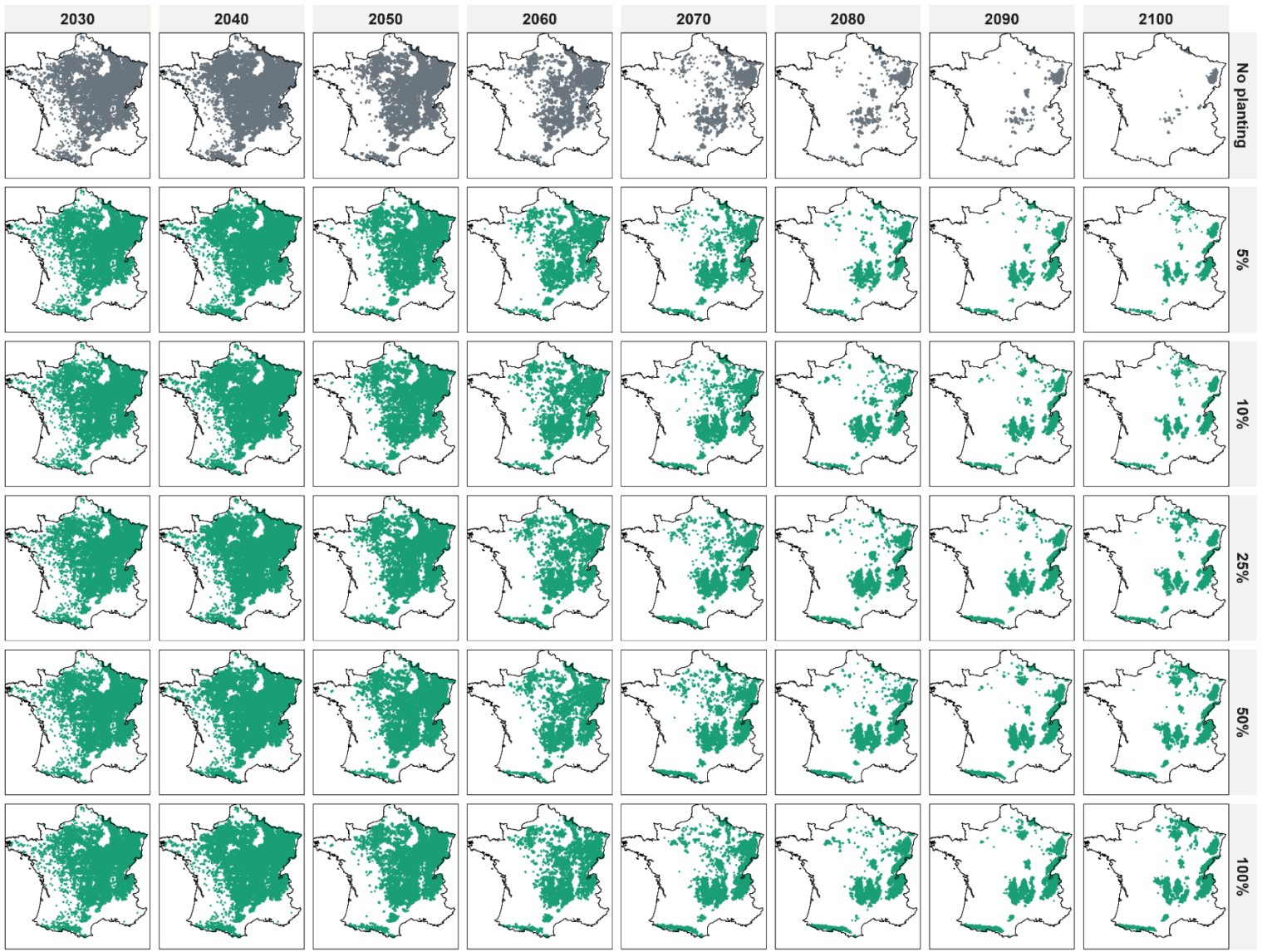

Figure S5. Maps of predicted *Q. petraea* presence from 2030 to 2100 simulated with *simRShift* under no planting and increasing planting efforts (5%, 10%, 25%, 50%, 100%).

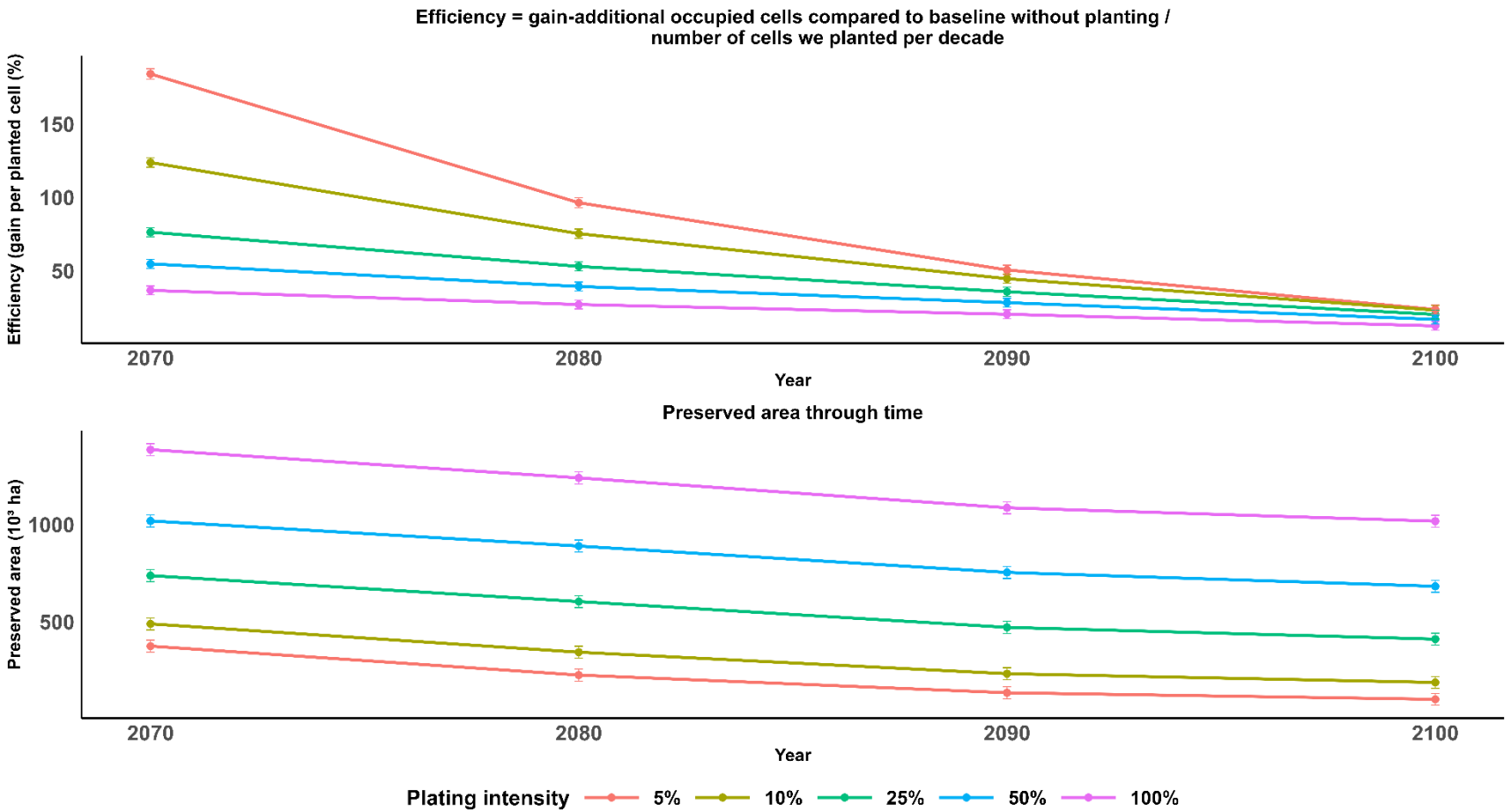

Figure S6. Temporal evolution of planting efficiency and total preserved area across planting efforts.
(Top) Planting efficiency, expressed as the gain in occupied cells relative to the no-planting baseline divided by the number of planted cells per decade.
(Bottom) Total preserved area through time for each planting-effort level.

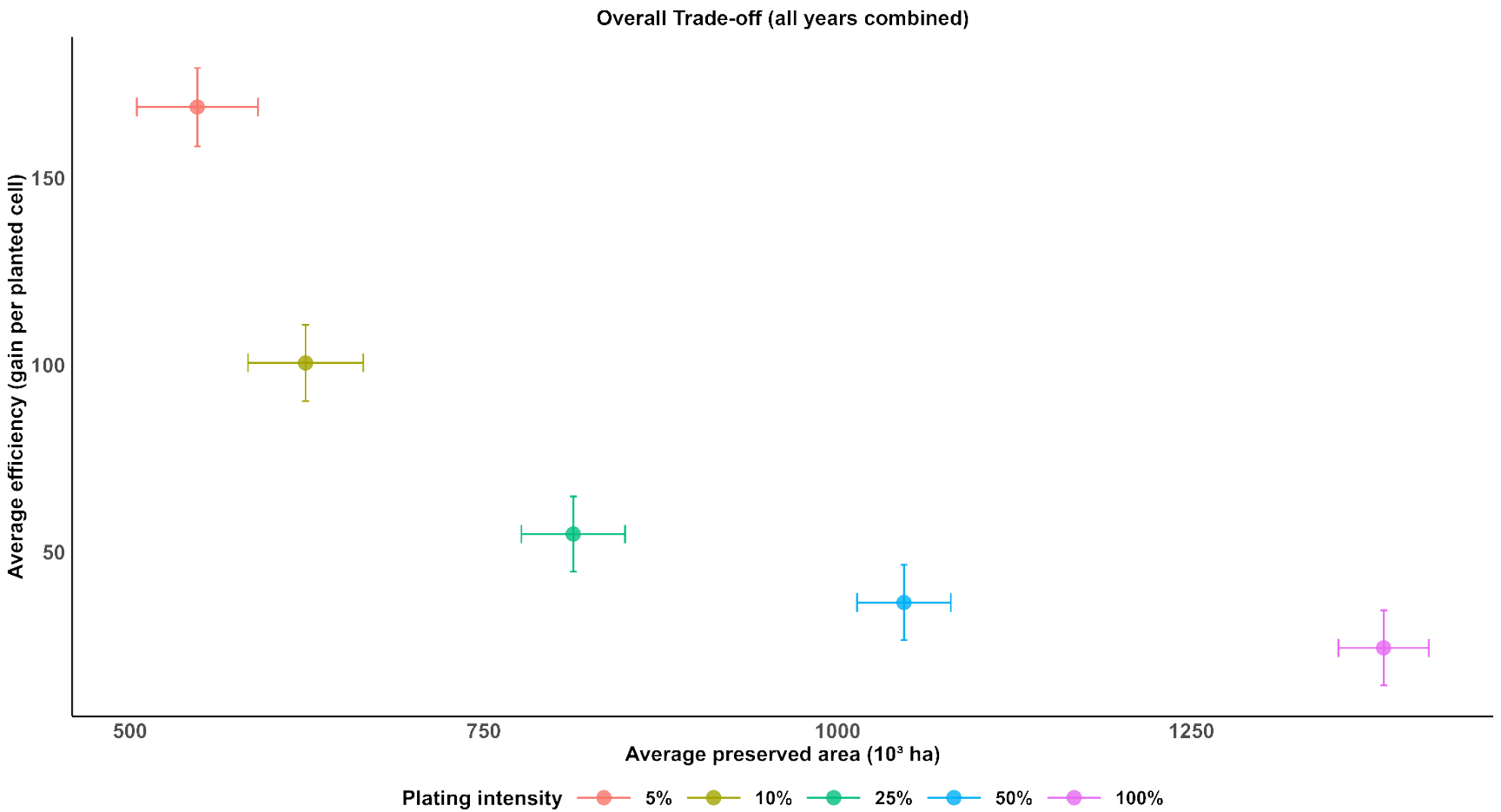

Figure S7. Trade-off between planting efficiency and total preserved area by 2100. Scatterplot showing the relationship between total preserved area (10^3 ha; x-axis) and planting efficiency (gain per planted cell; y-axis) across planting-effort levels. The concave relationship highlights diminishing returns: increasing planting effort increases absolute area preserved but reduces efficiency per planted cell.